MICROBIAL POPULATION STRUCTURE IMPACTS ANTIBIOTIC RESISTANCE

PRESENTED BY

NALIN J. M. RATNAYEKE

IN PARTIAL FULFILLMENT OF THE REQUIREMENTS FOR GRADUATION WITH DEAN'S SCHOLARS HONORS DEGREES IN BIOLOGY AND PHYSICS

PROF. VERNITA GORDON
SUPERVISING PROFESSOR

DATE

THE UNIVERSITY OF TEXAS AT AUSTIN
AUSTIN, TEXAS
MARCH 2015

I grant the Dean's Scholars Program permission to post a copy of my thesis on the University of Texas Digital Repository. For more information, visit:

http://repositories.lib.utexas.edu/about.

TITLE: MICROBIAL POPULATION STRUCTURE IMPACTS ANTIBIOTIC RESISTANCE

DEPARTMENTS: PHYSICS AND BIOLOGY

NALIN RATNAYEKE AUTHOR	DATE
PROF. VERNITA GORDON SUPERVISING PROFESSOR	DATE

SUPERVISOR:
Vernita D. Gordon

LOCATION:
Austin, Texas

DATE:
March 2015

ABSTRACT

Antibiotic resistance is an urgent and growing concern, and developing novel therapeutic approaches to overcome antibiotic-resistant infections has assumed immense significance. Recently, it has been shown that heterogeneity in a microbial environment can accelerate the development of antibiotic resistance. However, the effect of the spatial distribution of the microbial population itself remains to be investigated. Using the human pathogen *Pseudomonas aeruginosa*, we show that increasing cell density can drastically impact the survival and growth of antibiotic-resistant mutants in the presence of aminoglycoside antibiotics in a density-dependent manner. Increasing density confers both positive and negative effects to mutant survival, which we term "protection" and "inhibition", respectively. Using a combination of microbiological assays and biophysical modeling, we find that inhibition is mediated by a low-molecular weight, native by-product of bacterial metabolism that acts in conjunction with aminoglycosides through an effected increase in pH. A wide range of bacterial species are capable of producing inhibition, which is related to their growth by amino acid catabolism. We additionally develop a stochastic model of inhibition in homogeneous environments, which indicates that local density fluctuations on the scale of individual bacteria can significantly alter bacterial survival when colonizing a new environment. This work raises the possibility that the manipulation of population structure and the nutrient environment of microbes in conjunction with the use existing antibiotics could provide novel therapeutic approaches to combat antibiotic resistance.

PUBLICATIONS

Work included in this thesis has been published in:

- Kaushik, K.*, Ratnayeke, N.*, Katira, P., Gordon, V. (2015). The spatial profiles and metabolic capabilities of microbial populations impact the growth of antibiotic-resistant mutants. *J. R. Soc. Interface*: e20150018. Doi: 10.1098/rsif.2015.0018 * Co-first authorship
- Kaushik, K., Kessel, A., Ratnayeke, N., Gordon, V. (2015). A Low-Cost, Hands-on Module to Characterize Antimicrobial Compounds Using an Interdisciplinary, Biophysical Approach *PLoS Biol* 13(1): e1002044. Doi: 10.1371/journal.pbio.1002044

CONTENTS

LIST OF FIGURES

LIST OF TABLES

INTRODUCTION

Though advancements in medicine have led to the development of numerous antibiotics to treat bacterial infections, resistance to these antibiotics has become one of the primary issues in public health. In the United States alone, it is estimated that each year 2 million people contract resistant bacterial infections, from which at least 23,000 people die annually [1]. Understanding how populations of initially antibiotic-susceptible bacteria give rise to resistant strains is essential to designing treatment regimens that prevent or delay the development of antibiotic resistance, and to increasing the lifetimes of current lines of antibiotics [2–4]. Recently studies using experimental work and theoretical models have shown that heterogeneity in the environment (e.g. antibiotic gradients) can accelerate the evolution of genetically-based antibiotic resistance [5–10]. However, while these studies examine the variation in properties of the environment, they do not directly account for the effects of structure in the microbial population itself. Population structure includes properties such as the composition and spatial organization of multiple types of cells, and is highly relevant because most microbial communities consist of interacting, heterogeneous, multispecies populations [11]. Understanding these properties is vital to translating microbiological research, which is generally performed on simplified microbial communities consisting of uniformly distributed bacteria of a single strain, to more realistic and medically relevant systems.

Few studies to date have examined the effects of microbial population structure in the context of the development of antibiotic resistance [12–14]. An exception is found in research on microbial biofilms, multicellular aggregates embedded in an extracellular matrix on surfaces [15]. Typically, bacterial infections begin with a low-density inoculum of initially planktonic cells, which can subsequently develop into a chronic, biofilm infection [15]. The high cell density and microbial heterogeneity of biofilms have been shown to confer phenotypic antibiotic resistance to bacteria in biofilms, and can lead to recalcitrant infections [15]. However, the impact of microbial population structure on the development and propagation of *genotypic* antibiotic resistance remains to be explored. Unlike biofilm-based phenotypic antibiotic resistance, genetically-based antibiotic resistance can play a role in the microbial life cycle outside of biofilms, and has the potential to be inherited and spread to descendant populations.

In this work, we explore the impact of population structure on the manifestation of antibiotic resistance in *Pseudomonas aeruginosa*, a nosocomial pathogen which frequently affects burned, wounded, and ventilator-assisted patients, and also one of the leading proximate causes of death in patients with the

genetic disorder Cystic Fibrosis (CF) [16]. We find that increasing cell density can drastically impact the survival of antibiotic-resistant mutants generated in initially-susceptible populations of *P. aeruginosa* when exposed to antibiotics. In particular, we observe that increasing cell density can both positively and negatively impact resistant mutant survival, in a density and antibiotic concentration-dependent manner. We term these positive and negative effects on survival "protection" and "inhibition", respectively. This is seen at densities densities lower than those typically found in biofilms, and thus corresponds to densities found in initial infections. This phenomenon manifests itself in several systems, including those which are spatially-homogeneous and heterogeneous, and implies that the absolute number of antibiotic-resistant mutants that a population generates is not the sole determinant of the likelihood and extent of the spread of resistance. After phenomenologically describing these effects, we go on to elucidate the molecular mechanism of inhibition, and its potential ramifications for antibiotic resistance research.

We observe inhibition with two different aminoglycoside antibiotics: tobramycin, which is currently a front-line drug for treatment of *P. aeruginosa* infections, and gentamicin, which is commonly used in the treatment of a wide range of Gram-negative bacterial infections [17, 18]. Furthermore, we find that a wide range of microbial species can produce inhibition. Our results indicate that this is because the molecular agent of inhibition is a by-product of native bacterial metabolism, and that the mechanism of inhibition involves an alkaline change in the pH of the environment. This also implies that population structure can impact the development of antibiotic resistance through interactions between species in natural communities, in addition to through the spatial distribution of cells in an environment.

We develop a diffusion-based model with which we estimate the molecular weight of the molecular agent of inhibition, and we show the potential for this theoretical framework to be used in other contexts to help discover the identity of other inhibitory substances without the use of advanced equipment [19]. Additionally, informed by our observations and inferences about the mechanistic details of inhibition, we develop a stochastic model of inhibition in spatially-mixed systems. This model predicts that local fluctuations in cell density on the scale of individual bacteria could lead to our observations of inhibition in mixed systems, and implies that the spatial distribution of cells early on in the colonization of a new environment could lead to large divergences in community survival.

Combined, these results suggest that microbial population structure is a potentially powerful target and tool in developing novel therapeutic approaches to combat antibiotic resistance, and that the lifetime of current antibiotics might be extended with the use of natural products as synergistic agents. Furthermore, our finding that inhibition is mediated by a product of amino acid metabolism which acts through alkalinity suggests that modulation of micro-

bial metabolic state and environmental pH may be useful in the development of new therapies. A recent advance has shown that the addition of aerosolized bicarbonate to the CF lung can enhance the efficacy of innate antimicrobials [20, 21] and our results suggests that a similar approach could potentially enhance the efficacy of aerosolized aminoglycoside antibiotics. This work also introduces a novel interaction between members of microbial communities to be taken into account in ecological and medical studies on antibiotic resistance and community dynamics in general. Understanding these interactions is key to understanding how individual species and populations of bacteria, which have been well characterized in isolation, interact with each other in realistic natural and medical settings.

Part I

BACKGROUND

1

CELL DENSITY IMPACTS RESISTANT MUTANT SURVIVAL

This study was sparked by the serendipitous discovery that, when a heterogeneous population of antibiotic-resistant mutant and non-resistant wild-type (WT) *Pseudomonas aeruginosa* cells is exposed to aminoglycoside antibiotics, mutant survival depends heavily on aspects of population structure at the time of exposure, such as cell density and genetic composition. This phenomenon manifested itself in several different systems, which will be described in the following sections. These experiments paved the way for further investigations into the specific physical and biological mechanisms that govern these effects, which are described in Chapters 2 and 3.

1.1 PROTECTION AND INHIBITION IN SPATIALLY-MIXED SYSTEMS

We have found in a variety of systems that the ability of *P. aeruginosa* antibiotic-resistant mutants to survive antibiotic treatment is heavily modulated by population structure. This is most clearly seen when directly investigating the survival rate of mutant cells as a function of cell density. WT *P. aeruginosa* cells and a previously isolated resistant *P. aeruginosa* mutant (See methods for mutant characterization) were mixed together and plated on Luria-Bertani (LB) agar plates containing the antibiotic tobramycin at a concentration of 8 µg/mL, approximately 8 times the MINIMUM INHIBITORY CONCENTRATION (MIC) for the WT cells and slightly lower than MIC of the resistant mutant strain (9.6 µg/mL). The mixed population was created at a fixed mutant to WT ratio to simulate a naturally occurring mixed population of resistant and non-resistant cells, and was plated at cell densities varying over 4 orders of magnitude ($\sim 1 - 10^4$ cells/nL). WT cells would subsequently die on the agar and fail to form colonies, while some portion of the mutant cells would survive and grow into colonies which were then enumerated. Controls with only cells from the WT culture were plated at the same densities, and any spontaneously-generated mutants were subtracted from the colony counts.

MINIMUM INHIBITORY CONCENTRATION (MIC): *The minimum concentration of a given antibiotic which inhibits a microbe's growth.*

Each colony found on the plates after incubation was assumed to originate from a single cell inoculated on the plate which survived antibiotic exposure, such that colony counts represented the number of surviving mutant cells. Surprisingly, we found a non-monotonic dependence of this cell survival number on cell density at the time of plating (Fig. 1a). This reflects the observed maximum in the number of surviving cells and corresponding "sweet-spot" in cell density for mutant survival at approximately 10^3 cells/nL. Survival rates were calculated by dividing the colony counts by the known total number

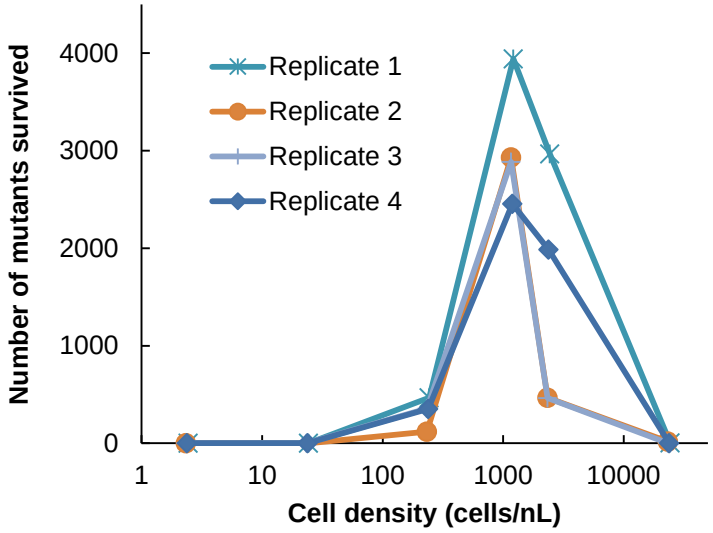

(a) Mutant survival numbers

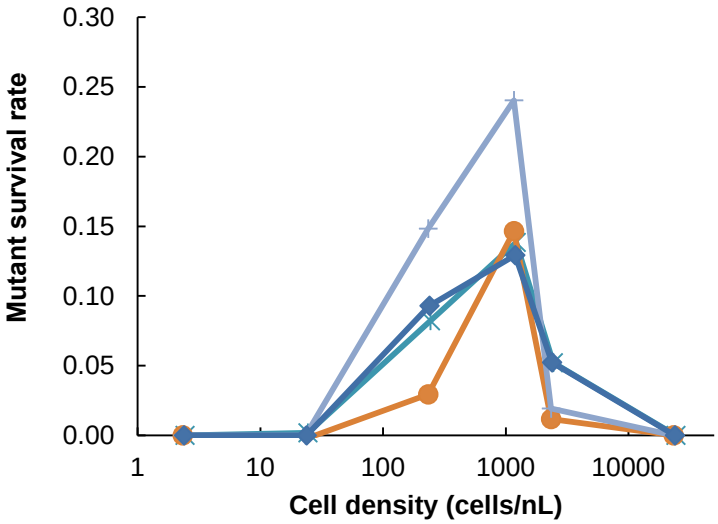

(b) Mutant survival rate

Figure 1: IN A SPATIALLY MIXED SYSTEM, THERE IS A NON-MONOTONIC DEPENDENCE OF RESISTANT MUTANT SURVIVAL ON CELL DENSITY. Antibiotic-resistant mutant cells were mixed with *P. aeruginosa* WT cells at fixed ratios, and plated on agar plates containing 8 μg/mL tobramycin at varying initial cell densities. We find that mutant survival both in absolute number (a) and in survival rate (b), is enhanced by increasing density at low densities, but is negated at high densities to an increasing degree. Replicates represent experiments performed on different days with fresh bacterial cultures.

of mutants plated at each density, and similarly the survival rate varied non-monotonically with cell density (Fig. 1b). This was unexpected, as it was not immediately obvious why the survival rate would vary in this way, or vary at all.

In a low cell density regime ($< \sim 10^3$ cells/nL), mutant survival was enhanced by increasing numbers of WT cells, and the presence of susceptible WT cells increased survival compared to mutant survival in isolation. However, this effect was negated to an increasing degree at high cell densities ($> \sim 10^3$cells/nL). The range of cell densities to which mutant survival responded varied over several orders of magnitude ($\sim 10^1 - 10^4$cells/nL).

PROTECTION: *The observed increase in mutant survival rate with increased cell density, which we see occur at relatively low densities.*

These results indicated that there may be counteracting phenomena which act to increase or decrease mutant survival in *P. aeruginosa*, which we term PROTECTION and INHIBITION, respectively. It is interesting to note the apparent maximum in survival rate and numbers, as well as the "sweet-spot" in cell density. In realistic populations, larger populations contain larger numbers of randomly-produced resistant mutant cells due to extra opportunities for cell division. In our system, however, simply increasing the number of cells in an antibiotic medium can counter intuitively decrease the number of surviving cells at high densities, or disproportionately increase the number of surviving cells at low densities. Thus, the gross number of antibiotic-resistant mutants in a population is not the sole determinant of a population's survival during exposure to aminoglycosides, and factors such as the total population size and the population density may be vital properties of natural bacterial populations.

INHIBITION: *The decrease in mutant survival rate with increased cell density, which we observe at relatively high densities.*

1.2 SOME THOUGHTS ON PROTECTION

We define protection as an observed increase in mutant survival rate with increasing cell densities. In the experiment described in the previous section, protection was seen at relatively low cell densities, while inhibition was seen at high ones. While the focus of this thesis is on inhibition, a few aspects of protection are worth noting. Phenomena analogous to protection have been investigated in the literature, primarily in two forms: biofilms and the inoculum effect.

1.2.1 *Biofilms*

BIOFILMS are high density aggregates of bacteria which form on surfaces which tend to display increased resistance to antibiotics [15]. While the mechanisms by which this occurs are not well understood, it is thought that decreased diffusive penetration of the biofilm by antibiotics, and metabolic changes triggered by oxygen and nutrient deprivation could be potential causes [15]. However, biofilm densities are typically much higher than those seen with protection.

BIOFILMS: *High density surface aggregates of bacteria characterized by resilience to antibiotic exposure.*

The protective effect in this system is seen well below 10^2 cells/nL, corresponding to average distances between cells on the order of tens of cell lengths, which is lower than one would expect to cause barriers to antibiotic diffusion and oxygen and nutrient depletion.

Interestingly, inhibition occurs in cell densities of the same order of magnitude as those found in biofilms. This indicates that the molecular mechanism behind inhibition either is not active in biofilm environments, or is present and compensatory mechanisms exist in biofilms which counteract it. The latter possibility is particularly interesting, as these compensatory mechanisms could be targeted during treatments to eradicate or inhibit biofilm formation. It is unclear presently which of these possibilities is true, though results in Chapter 3 seems to point to the latter, and further studies will need to be performed.

1.2.2 *The inoculum effect*

Protection seems to be more similar to the INOCULUM EFFECT. The inoculum effect is a well documented observation that in general, cell density alters measured MIC values when tested in liquid culture [13]. In particular, higher densities tend to produce higher readings of the MIC for a given organism. Similarly to biofilm resistance, the inoculum effect is not currently well understood, however it is hypothesized that antibiotic degradation or differences in the molar quantities per cell of the antibiotic may be responsible [13]. Studies into the inoculum effect show it manifesting in systems with the same order of magnitude cell density that we see protection[12, 13], which may indicate a common molecular mechanism between the two. In particular, the mechanism of reductions in the molar quantities of antibiotics per cell leading to increased antibiotic resistance is applied to develop a model of inhibition in spatially-mixed systems in Chapter 4.

INOCULUM EFFECT: *The observed increase in measured MIC values with increased culture density.*

1.3 DECONVOLVING INHIBITION FROM PROTECTION

Under the experimental conditions described in Section 1.1, we observe both protection and inhibition, and it is unclear whether they govern two exclusive density ranges, or both act in varying degrees in overlapping ranges. In order to deconvolve inhibition from protection, a slightly altered experiment was performed. In this experiment, the tobramycin concentration of the LB agar growth medium was lowered to 4 µg/mL. This decision was based on the inference that protection would be diminished at lower antibiotic concentrations due to decreased stress. In other words, we expected that lowering the concentration of antibiotics would remove the dependence of cells on protection to survive.

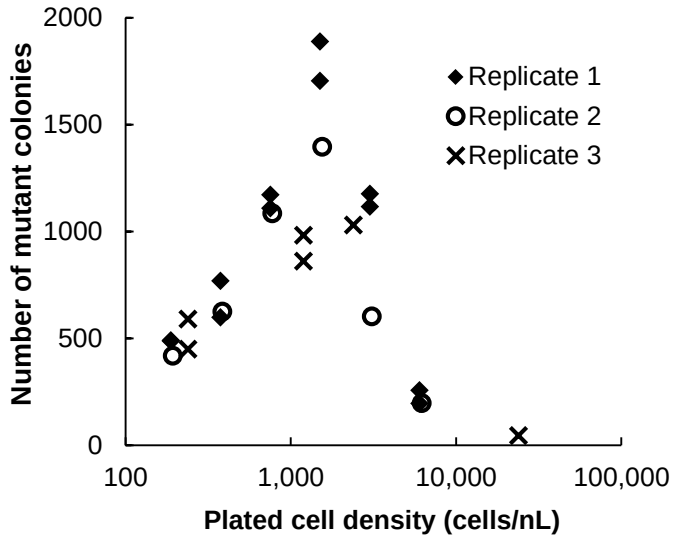

(a) Number of mutant colonies

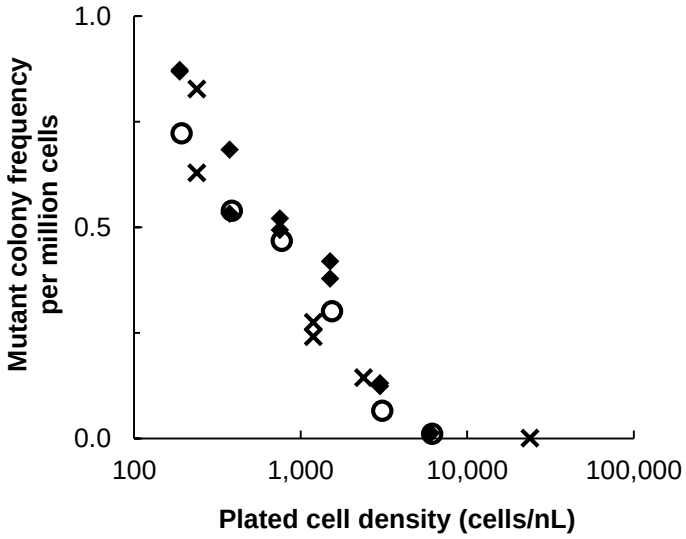

(b) Mutant colony frequency

Figure 2: ADJUSTING ANTIBIOTIC CONCENTRATION CAN DECONVOLVE INHIBITION FROM PROTECTION. Cells from a *P. aeruginosa* WT overnight culture with non-resistant cells and spontaneous antibiotic-resistant mutants were plated on agar plates containing 8 μg/mL tobramycin at varying initial cell densities. We find a non-monotonic dependence of the number of mutant colonies formed on cell density (a), while we find a monotonic decrease in the mutant colony frequency (defined to be the number of mutant colonies divided by the total number of cells plated) (b). Replicates represent experiments done on different days with fresh bacterial cultures. Figure adapted from [22].

The lower antibiotic concentration at only 4 times the MIC of the WT increased the number of random mutants that appeared in overnight cultures of WT cells which could survive antibiotic exposure on the plate, and enumeration of added-in isolated mutant strains became difficult. As a result, overnight WT cultures alone were plated onto the antibiotic plate. WT cells would again die when exposed to antibiotics, however random mutants which appeared in the overnight culture survived and formed colonies.

In accordance with the inference, the protective effect was no longer seen, and we observed a monotonic decrease in survival rate (Fig. 2b). While survival rate was not directly observable in this experiment, due to the fact that the true mutant cell number in the population was unknown, the observed MUTANT COLONY FREQUENCY (number of mutant colonies/total cells plated) is equal to the survival rate times the true mutant cell frequency, and is thus directly proportional to mutant survival rate.

MUTANT COLONY FREQUENCY: *Number of mutant colonies/total cells plated. Proportional to the survival rate.*

At 8 µg/mL tobramycin the survival rate began low and increased to a maximum at $\sim 10^4$ cells/nL. However, in this experiment at 4 µg/mL, survival rate began at its maximum at the low density of 50 cells/nL, consistent with the idea that cells no longer needed protection in order to survive, and decayed with increasing cell density. Thus, experiments performed at 4 µg/mL allow us to examine inhibition in isolation.

A survival rate of this form still led to a non-monotonic trend of the total number of mutants which survived on the antibiotic plate (Fig. 2a) , and indicates that even without two counteracting forces which act on cell survival, a maximum number of surviving cells and corresponding optimal cell density for survival can still be observed. This stems mathematically from the fact that the number of mutant colonies which grow on the plate is the product of the number of mutants plated, and the survival rate on the plate. As cell density increases, the total number of mutants plated linearly increases, while at the same time the survival rate decreases. The product of these two opposite trending functions can contain a maximum.

1.4 SOURCE-SINK DYNAMICS: A CASE-STUDY

While investigating evolution in SOURCE-SINK SYSTEMS, we observed that mutant survival numbers were not self-consistent under the assumption that cell density does not impact survival probability, which is consistent with our previously described results. In these systems, organisms in a source environment, to which they are well adapted, are connected by migration to a sink environment, to which they are maladapted. Only through mutation can the organism adapt to populate the sink environment. In these investigations, we experimentally tested a computational model of source-sink systems which predicted the

SOURCE-SINK SYSTEM: *Ecological system in which a population is free to migrate between an environment it is well-adapted to and one it is not.*

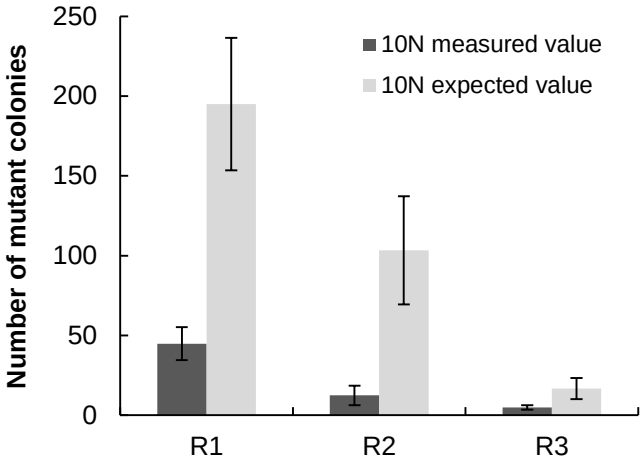

Figure 3: THE NUMBER OF CELLS WHICH SURVIVE MIGRATION TO SINK IS NOT PROPORTIONAL TO THE MIGRATION RATE.We passaged cells from an antibiotic-free source to an antibiotic containing sink over the course of several days with varying migration rates (number of cells/day). When antibiotic-resistant mutants arrived in the sink, we found that fewer cells appeared on the plate at higher migration rates than we would expect from numbers at lower migration rates. Replicates represent different source cultures, each of which was migrated to a sink with N and 10N cells. Expected value of 10N was calculated from measured values of N.

average time of adaptation of an organism to a harsh environment as a function of various parameters such as mutation and migration rate [7].

To test the predictions of this model, migration between a source and sink was simulated by passaging *P. aeruginosa* from an antibiotic-free culture to an LB agar growth medium containing the tobramycin at 8 µg/mL over the course of several days to weeks. Since the antibiotic concentration in the sink is approximately 8 times the minimum inhibitory concentration (MIC) of the WT, growth was not seen in the sink until a resistant mutant arrived from the source culture. The amount of time until a mutant cell arrived in the antibiotic medium and survived was taken as the time of adaptation, which the model quantitatively predicted.

To determine how migration rate impacted the time of adaptation experimentally, the number of cells transferred to the sink environment, which is proportional to the migration rate, was varied over an order of magnitude. $N = \sim 10^8$ cells and 10N cells from source cultures were plated onto antibiotic plates over the course of several days, and when a mutant strain arose in the source and was migrated to a sink, we found that plates with N cells and 10N cells did not contain a proportional number of mutants, despite the fact that an approximately proportional number of mutants would have migrated

to the sink from the same source culture (Fig. 3). Instead, the observed frequency of mutants (number of mutant colonies/number of cells plated) was much higher in the lower cell density plates (N cells plated) than in higher cell density plates (10N cells plated), and repeated consistently over multiple days and replicates.

These results indicated that the adaptation of the *P. aeruginosa* cells to the sink environment not only depended on obvious parameters such as mutation rate, which would alter the number of mutants generated, and migration rate, but also on cell density in the sink following migration. While higher migration rates could lead to an increased number of mutants migrating to the sink, it also leads to increased average cell densities in the sink and thus potentially nets a decrease in mutant numbers.

While adaptation time was not extensively compared at multiple migration rates, a trend was seen that intermediate migration rates, which could correspond to plating densities of maximal survival rate, seemed to result in mutants surviving in the sink at approximately the same time or before migration rates which were an order of magnitude larger. In this system, while a higher migration rate increased the likelihood of a resistant mutant arriving in the sink environment to populate it, the resulting increased cell density on the antibiotic-containing plate decreased the likelihood of survival of these mutants.

As a result, inhibition and protection may manifest themselves not only in homogeneous populations which are uniformly exposed to antibiotics, but also spatially-heterogeneous populations, and may lead to altered ecological and evolutionary dynamics in these systems. Many realistic bacterial populations of both scientific and medical relevance display spatial heterogeneities, and thus it is important to examine our observed phenomenon in this system, and in other relevant systems.

Part II

PHYSICAL AND BIOLOGICAL DESCRIPTION OF INHIBITION

2

PHYSICAL DESCRIPTION OF INHIBITION

The remainder of this thesis will primarily deal with the phenomenon of inhibition, in which *Pseudomonas aeruginosa* mutant cell survival decreases with increasing cell densities when exposed to antibiotics. While inhibition was seen in several different contexts, we also sought to determine the physical mechanisms which were responsible for it. Several experiments were performed which aimed to elucidate the physical properties of inhibition, and a physics-based diffusion model of inhibition in a spatially-heterogeneous system was developed to further characterize this phenomenon.

2.1 INHIBITION ACTS AT A DISTANCE

Since there were orders of magnitude more WT cells than antibiotic resistant mutant cells in the experiments described in Chapter 1, we hypothesized that WT cells were inhibiting antibiotic-resistant mutants. To investigate the role of WT cells in inhibition, antibiotic-resistant mutants were overlaid onto LB agar growth medium containing 4 or 8 µg/mL tobramycin, and WT cells were deposited onto filter-paper discs placed on this background. This assay was inspired by the antibiotic DISC-DIFFUSION ASSAY, often used to evaluate susceptibility to antibiotics [23]. After incubation of the antibiotic-resistant mutant background, regions of clearing or ZONES OF INHIBITION surrounding the filter discs in which there was no visible mutant growth were seen at both concentrations (Fig. 4).

DISC-DIFFUSION ASSAY: *Filter paper discs imbued with cells or antibiotics are placed on agar plates with a background of cells. Molecules diffuse out from the disc and form zones of inhibition.*

ZONE OF INHIBITION: *Clearing in bacterial growth observed around a source of inhibitory substance after incubation.*

These results indicated that WT cells indeed were capable of inhibiting the growth of resistant mutant in the presence of antibiotics. This is a remarkable finding, as many other instances of bacterial inhibition in general involve competition between different species, or between different lineages within a given species. The inhibition which we observe is between mutant strain and its recent progenitor strain.

Additionally, this effect works at a distance. Experiments described in Chapter 3 confirmed that inhibition was not due to nutrient depletion or cell-to-cell contact, and combined with the discovery of zones of inhibition, indicate that inhibition is mediated by a diffusible inhibitory factor (IF). These results are consistent with those in the mixed-system experiments in Chapter 1. Assuming cells produce a relatively constant amount of the IF, increasing cell density would increase the concentration of IF in the media, and could lead to the observed decrease in cell survival.

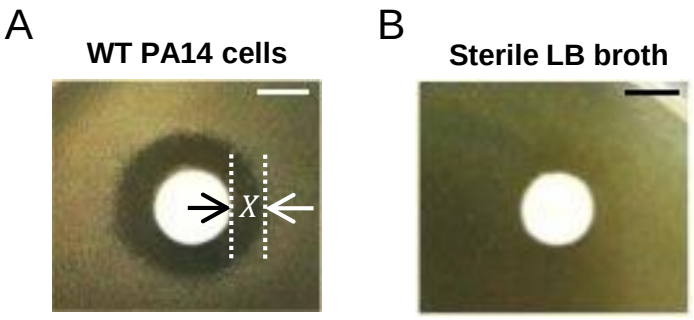

Figure 4: WT PA14 CELLS INHIBIT THE GROWTH OF RESISTANT MUTANTS IN THE PRESENCE OF TOBRAMYCIN. We deposited $\sim 10^9 - 10^{10}$ WT *P. aeruginosa* cells onto filter paper discs on 4 or 8 μg/mL tobramycin LB agar plates which were inoculated with antibiotic-resistant *P. aeruginosa* cells. We find that zones of inhibition are formed around the cells after incubation (A). We see that sterile LB media which is used for overnight culturing of the WT cells does not cause inhibition, and similar results are seen when overnight supernatant is deposited on the disc as well (B). The size of the inhibition zone is represented by X, the perpendicular distance between the edge of the disc to the edge of the zone. Scale bars are 5 mm. Figure adapted from [22].

2.2 MODELING OF INHIBITORY FACTOR DIFFUSION

To determine the diffusive characteristics of the IF, an analytical model of the disc-diffusion assay was developed. This model built upon quantitative theory describing antibiotic disc-diffusion assays [24]. Since antibiotic disc-diffusion assays share the same geometry and general characteristics (an inhibitory substance which diffuses from a source) as our system, these models were a reasonable base.

2.2.1 *Theoretical basis for disc-diffusion assays*

For antibiotics and other inhibitory substances, models of the disc-diffusion assay conform to the following general scheme. An inhibitory substance from a localized source diffuse out into agar which is inoculated with bacterial cells. This diffusion can be represented by a concentration profile of the substance which varies with distance from the source and time. Cells which are exposed to a concentration higher than a threshold concentration die and fail to form visible growth after incubation. Since higher source concentrations in general increase the concentration at a given point, and decrease the time it takes for

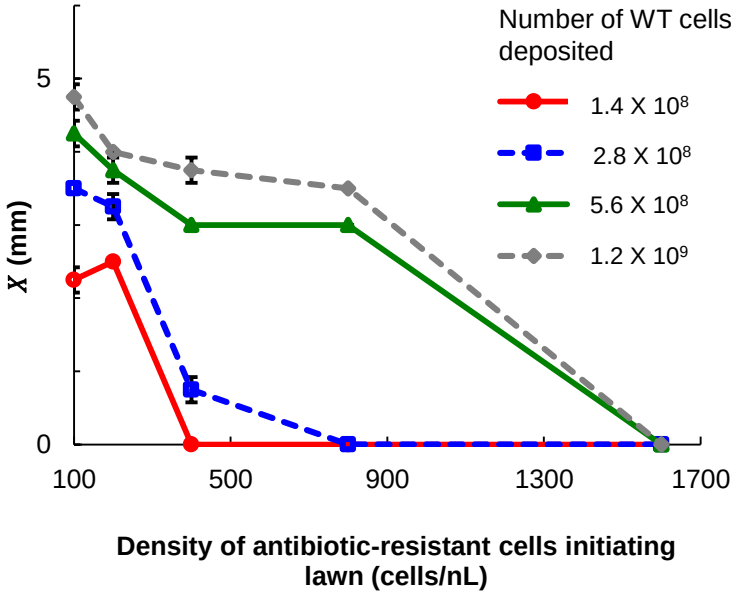

Figure 5: INCREASING THE INITIAL DENSITY OF MUTANTS IN THE LAWN DECREASES ZONE SIZE. Varying numbers of WT and mutant cells were used on the disc and on the agar lawn respectively under the same conditions as Figure 4. We observe that the size of the inhibition zone increases with increasing numbers of WT cells on the disc, and decreases with increasing numbers on the lawn. For each point, N = 3. Figure adapted from [22].

the concentration at a given point to reach a given value, increasing the source concentration increases the range at which cells die, and thus the zone size. In accordance with this, when we increase the number of WT cells on the disc, the inhibition zone size X (the distance between the edge of the disc and the edge of the zone) increases.

Empirically, it has been observed that the survival of cells exposed to antibiotics depends on the time since inoculation not only implicitly, because the concentration profile depends on time, but also explicitly. Studies have shown that after a CRITICAL TIME (T_c) of growth, cells are not cleared, regardless of the concentration they are exposed to[25]. This time of growth corresponds corresponds to cells on the lawn growing to a critical density which prevents the clearing of cells by the antibiotics [24, 26, 27]. We see this effect in our system when we alter the initial inoculum on the agar plate. As the density increases, the zone size decreases, which can be explained by a lowering of the incubation time it takes for the lawn to reach the critical density (Fig. 5).

CRITICAL TIME (T_c): *The amount of time of growth after which cells on the lawn do not die and the zone size is set.*

Though no conclusive work has been done to fully elucidate it, this phenomenon could be another manifestation of the underlying cause of our observations of protection and also of the inoculum effect. In certain density

regimes, higher densities could lead to increased resilience to antibiotics, and thus this critical density the lawn needs to reach to survive could correspond to the density which confers a large degree of resilience. Mechanistically it is difficult to say what causes this, but it has been proposed that antibiotics at the diffusive front are uptaken at a higher rate than they are replenished, and thus are diffusion limited [27]. Regardless, this phenomenon has been routinely seen in antibiotic disc-diffusion assays, and is considered a vital component of models which try to describe them.

2.2.2 *Model of inhibition in a disc-diffusion assay*

With the framework from the previous section in mind, we modeled the relationship between zone size and number of cells on the disc. While there are several different models which describe slightly different antibiotic disc-diffusion assays, with different sizes and natures of the antibiotic source (e.g. whether the concentration at the disc falls or stays constant)[25], we use aspects of these models to most accurately describe our system. Since the IF we observe likely behaves no differently than an antibiotic, we expect these models to be a reasonable starting point for our investigations. We assume:

1. Cells release a set amount of IF to a concentration $[IF]_0$ at the disc
2. The IF obeys Fick's laws of diffusion and diffuses out of the disc with a constant diffusion coefficient D and no consumption or degradation
3. A threshold IF concentration $[IF]_c$ is required to kill or prevent future growth of mutant cells
4. IF does not cause inhibition of cells after a critical time T_c of incubation (i.e. the zone size is set at this time).

We assume that the IF is not significantly consumed or degraded as it diffuses out and comes in contact with cells. While this does not have to be the case in reality, most antibiotic disc-diffusion models assume this and constitutes what would likely be a minor perturbation from a model which takes it into account the possibility.

In this system, a finite quantity of IF is released by cells at the disc and diffuses into a cylindrical agar volume with radius much greater than height (Fig. 6). The diffusion of the IF can be described by Fick's Law of Diffusion:

$$\frac{\partial[IF]}{\partial t} = D\nabla^2[IF] \tag{1}$$

where [IF] is the concentration of IF at a given point and time.

A system with this geometry has been solved with a non-closed form solution [28]. However, this solution has been shown numerically to be approximated by the solution of one-dimensional diffusion from a constant source [28].

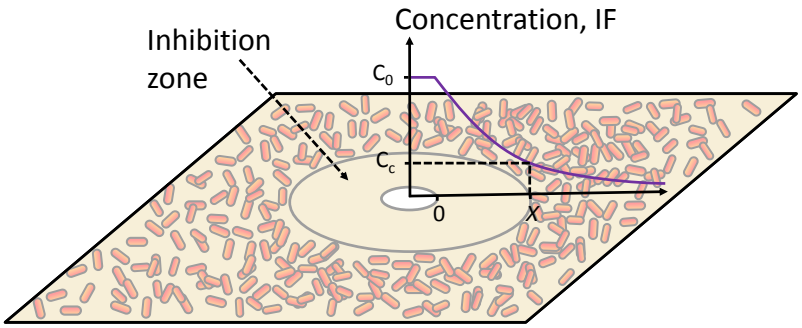

Figure 6: SCHEMATIC OF DISC-DIFFUSION MODEL. Antibiotics diffuse out from the disc and establish a concentration profile (purple line) which evolves with time. At the critical time, the point X at which the concentration of IF is C_c is set as the zone boundary.

The concentration profile of IF as a function of distance from the disc x and time after inoculation and placement of the disc t, can thus be approximately described in our system by:

$$[IF] = \frac{[IF]_0}{4\pi Dt} \exp\left(-\frac{x^2}{4Dt}\right) \tag{2}$$

The size of an inhibition zone can be quantified by the distance between the edge of the zone and the edge of the disc, which we call X (Fig. 4). At the critical time, T_C, the zone size X is set at a value equal to the lowest x with concentration equal to $[IF]_c$. Since the concentration profile is monotone for all t, all x greater than this have $[IF] < [IF]_C$ and cells survive, while all x less than this have $[IF] > [IF]_C$ and cells are inhibited. Thus, X must satisfy the expression

$$[IF]_c = \frac{[IF]_0}{4\pi DT_c} \exp\left(-\frac{X^2}{4DT_c}\right) \tag{3}$$

Rearranging this gives

$$X^2 = 4DT_c \ln[IF]_0 + F([IF]_c, D, T_c) \tag{4}$$

where F is a function which does not depend on $[IF]_0$. This expression would be true, regardless of whether cells release an inhibitory factor at the disc, or if antibiotics or some other inhibitor substance was imbued onto the disc. If the inhibitory factor is released sufficiently fast from cells placed on the disc, we can model cell-produced IF using this expression. This is a reasonable assumption to make, since WT cells are capable of producing it and die soon after being exposed to antibiotics. Assuming $[IF]_0$ is proportional to the num-

ber of cells N_0 inoculated onto the disc (i.e. $[IF]_0 = k_0 \times N_0$ where k_0 is a production constant), Eq. 4 becomes

$$X^2 = 4DT_c \ln(N_0) + F(N_c, D, T_c) \tag{5}$$

where N_c is the minimum number of cells on the disc required to produce a visible zone of inhibition. At numbers below this, the cells do not produce a high enough concentration to kill surrounding antibiotic-resistant mutants. Notably, this expression implies a linear relationship between X^2 and $\ln(N_0)$, with a linear coefficient equal to $4DT_c$. Therefore a linear regression of X^2 and $\ln(N_0)$ can be used to estimate the diffusion coefficient D if T_c is known. While relevant factors such as N_c(and the corresponding $[IF]_c$) likely change with changes in antibiotic concentration on the agar plate, and T_c likely would change with any factor which impacts the time it takes to reach the critical density[1], the analysis and estimate of D, which is not dependent on any of those, should not change.

T_c for a given set of growth conditions can be estimated by PREINCUBATING lawns for varying amounts of time before placing discs on the plate [27]. Since $T_c$is the time it takes for the inoculated bacteria to reach the critical population size, preincubation for a time h changes Eq. 5 to

$$X^2 = 4D(T_c - h)\ln(N_0) + F(N_c, D, T_c) \tag{6}$$

PREINCUBATION: *Alteration to the disc-diffusion assay where the inoculated cells on the agar are allowed to grow prior to placing the disc on the plate.*

As h increases, the density of cells on the lawn increases due to bacterial growth, and X^2 should decrease. When $h = T_c$, we expect X^2 to equal zero. These inferences are consistent with the results in Figure 5, where zone size decreases down to zero with increasing numbers of cells on the lawn initially. Within this theoretical framework, we can estimate the diffusion coefficient of the IF.

2.3 EXPERIMENTAL MEASUREMENT OF INHIBITORY FACTOR DIFFUSION CHARACTERISTICS

Since our model is dependent on the concept of a critical time, we sought to confirm qualitatively that this is the case with inhibition. The critical time is equal to the amount of time it takes for the lawn density to increase from its initial inoculation to the critical density, and thus increasing the initial lawn density should decrease this time and in essence imparting a non-zero h. Experimentally, we see this to be the case (Fig. 7b). Therefore critical time is likely relevant in our system and the developed model can be used to describe the IF.[2]

1 e.g. temperature, initial inoculum size, growth medium and antibiotic concentration.

2 The cells on the plate are at a relatively low density (~50 cells/nL), and thus are at a density much lower than those we see inhibition in. Therefore we would not expect an increase in lawn

We varied the number of cells placed onto the disc in the disc-diffusion assay at 4 µg/mL tobramycin, and found the predicted linear relationship between X^2 and $\ln(N_0)$(Fig. 7a). We found T_c to be 108 ± 26 minutes by measuring zone sizes from plates which had been incubated for varying amounts of time before disc placement and estimating the $X^2 = 0$ intercept using linear regression. From this, and the estimated linear coefficient of the regression from Figure 7a, we estimate D to be $4.5 \pm 0.5 \times 10^{-6}$ cm²/s and N_c to be $2.1 \pm 6.3 \times 10^6$cells.

2.3.1 *The inhibitory factor is a molecule of low molecular weight*

While the diffusion coefficient for the IF is a physically useful valuable quantity to estimate, it also allows us to infer the molecular weight of the IF, which is crucial for identifying the molecule. According to the Stokes-Einstein relation, the diffusion coefficient of a spherical molecule in a fluid is given by

$$D = \frac{k_B T}{6\pi\eta R} \tag{7}$$

, where k_B is Boltzmann's constant, T is the temperature of the fluid, η is the viscosity of the fluid, and R is the radius of the molecule. Approximating the diffusing molecule to be spherical, it is easy to show that

$$D = \frac{4\pi\rho}{3}\frac{k_B T}{6\pi\eta} MW^{-\frac{1}{3}} \tag{8}$$

, where molecular weight of the molecule MW and average density ρ satisfy $MW = \frac{4}{3}\pi R^3 \rho$. If we measure the diffusion coefficient of IF of a molecule of known molecular weight at the same conditions (i.e. the same T and η) and assume the molecules have the same ρ, we can approximate the IF molecular weight by

$$MW_F = MW_A \left(\frac{D_A}{D_{IF}}\right)^3 \tag{9}$$

,where MW_A and D_A are the molecular weight and diffusion coefficient of the known molecule respectively.

To ensure that the conditions under which we measure the diffusion of the known molecule were the same as those for the IF, we chose the known

density to increase the lawn susceptibility to the tobramycin on the plate. However, the cells on the disc are effectively at high density, and thus cells in the lawn surrounding the disc are exposed to the equivalent [IF] of high densities and are inhibited. With a system organized like this, an increase in lawn density confers the benefits of protection without significantly changing the amount of IF cells are exposed to.

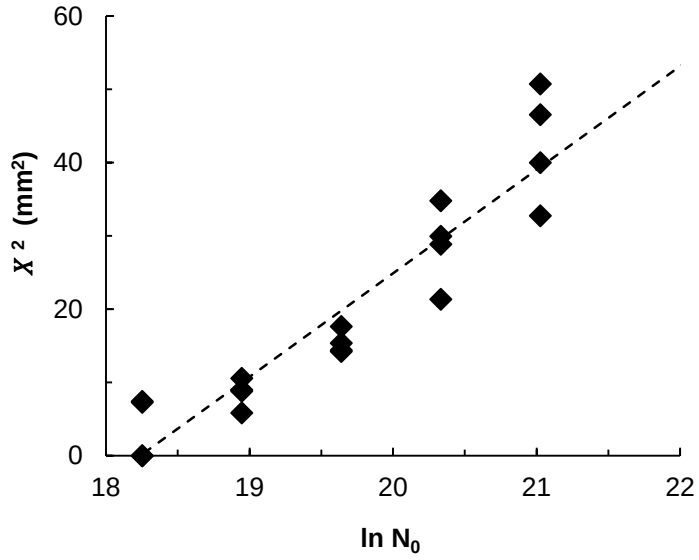

(a) Zone size as a function of cells on disc

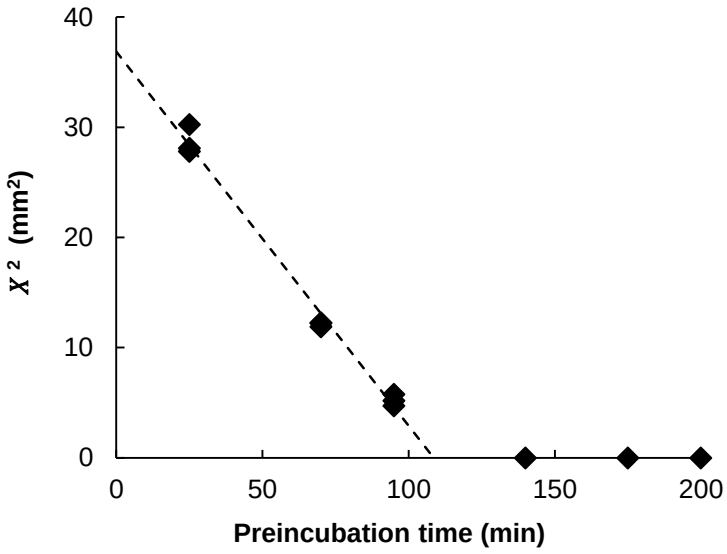

(b) Zone size as a function of preincubation time

Figure 7: EXPERIMENTAL RESULTS OF DISC-DIFFUSION MATCH MODEL PREDICTIONS. a) When we vary the number of cells N_0 on the disc under the same conditions as Figure 4, we find that the zone size squared (X^2) varies linearly with $\ln N_0$ ($R^2 = .87$, $N = 4$). b) When we preincubate lawns for varying times, we find a linear decrease in X^2, down to zero ($R^2 = .99$, $N = 3$) and we estimate the value of T_c to be 108 ± 26 min. Figures adapted from [22].

molecule to be tobramycin ($MW = 467.5$), and performed an analogous experiment to the inhibition disc-diffusion assay. In this antibiotic disc-diffusion assay, we placed discs with varying concentrations of tobramycin on antibiotic-free LB agar inoculated with WT cells. Tobramycin would diffuse out from the disc and produce zones of inhibitions in the lawns after incubation. A similar expression to Eq. 6 can be written for tobramycin (Tob):

$$X^2 = 4D\,(T_c - h)\ln[Tob]_0 + F([Tob]_c, D, T_c) \tag{10}$$

Therefore the same analysis which we performed for inhibition can be used to determine the diffusion coefficient of tobramycin in our system. We found T_c to be 680 ± 50 minutes and estimatedD_{Tob} to be $9.6 \pm 0.8 \times 10^{-7}$ cm²/s.

Using these results and Eq. 9, we estimate the molecular weight of IF to be 6 ± 3 Da, indicating it is a small molecule. We additionally performed the same experiments for measuring the diffusion coefficient of the IF on 8 µg/mL tobramycin plates, to examine the reproducibility of our molecular weight estimate. While altering the antibiotic concentration could change both T_c and N_c, theoretically D and the resulting estimated molecular weight should not change. We find the measured D to be$2.5 \pm 0.4 \times 10^{-6}$ cm²/s, with a corresponding molecular weight estimate of 37 ± 23 Da. The measured N_c at this concentration was $1.6 \pm 3.7 \times 10^6$ cells, which is approximately 75% of this value at 4 µg/mL, suggesting that there is an increased sensitivity to the IF at higher tobramycin concentrations.

2.3.2 *Overview of modeling results and limitations*

The estimates of D and the molecular weight at 8 µg/mL tobramycin are relatively close to measurements at 4 µg/mL tobramycin, and indicates that the IF molecular weight may be near the lower limit of what can be estimated using this model and experimental approach. More experimental work must be done to fully validate the accuracy of this model under these conditions. In particular, rather than using one molecular weight standard to estimate the molecular weight of IF using Eq. 9, Eq. 8 can be rearranged to

$$MW = \left(\frac{4\pi\rho}{3}\frac{k_B T}{6\pi\eta}\right)^3 D^{-3} \tag{11}$$

, suggesting a linear relationship between MW and D^{-3}. This was assumed to be true in the aforementioned analysis. By measuring the D of various other antibiotics and bactericidal chemicals which produce zones of inhibition using the disc-diffusion assay, a regression of known MW and measured D^{-3} can

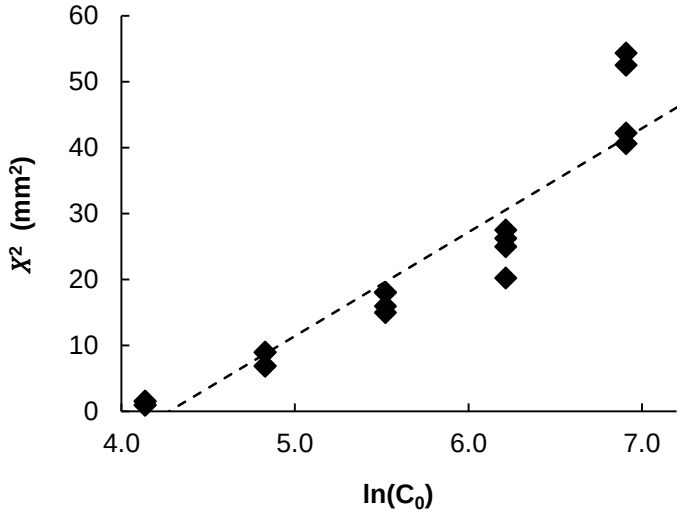

(a) Inhibition zone size as function of tobramycin concentration

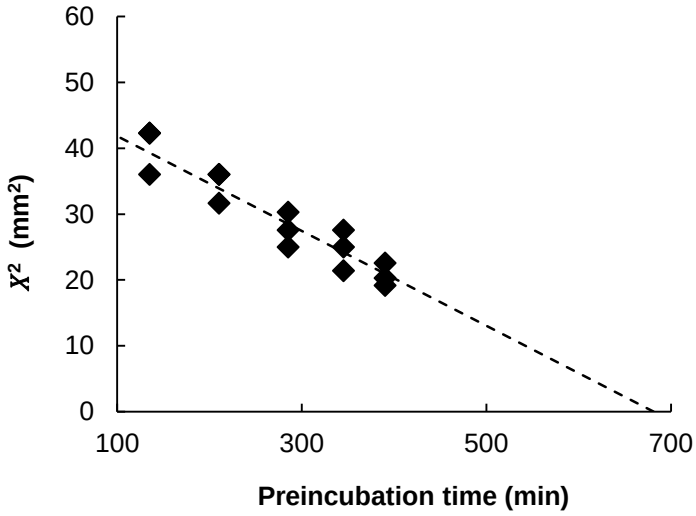

(b) Inhibition zone size as function of preincubation time

Figure 8: MODELING DIFFUSION OF TOBRAMYCIN. a) Increasing concentrations of tobramycin were deposited on WT PA14 inoculated lawns on antibiotic-free LB agar. We find that the zone size squared (X^2) varies linearly with $\ln C_0$ ($R^2 = .89$, $N = 4$). b) When we preincubate lawns for varying times, we find a linear decrease in X^2, down to zero ($R^2 = .93$, $N = 4$) and we estimate the value of T_c to be 680 ± 50 min. Figures adapted from [22].

be performed. Not only could the assumption of linearity be verified experimentally, but the linear coefficient of this regression could be used to more accurately predict the molecular weight of the IF, as well as improve confidence interval estimates.

The theoretical framework described in this section can also be used in other contexts in order to aid in the discovery of other inhibitory substances. Natural products (i.e. substances that are produced by organisms such as plants and microbes) are commonly used as antibiotics or antibiotic precursors, and current active research still involves assays similar to the disc-diffusion assay to determine if microbes produce inhibitory substances of medical value. This assay and model is a technique which does not require the use of expensive equipment, and may be a useful too in these studies, especially in third-world countries with limited resources [19].

While future work into the disc-diffusion model will further elucidate the diffusive properties of the IF and the accuracy of the model, our results at present represent an order of magnitude estimate of the IF molecular weight that indicate that the IF is a relatively small molecule. While the molecule is unlikely to be less than 10 Da (smaller than the molecular weight of most biologically relevant molecules), as predicted with experiments performed at 4 µg/mL, the order of magnitude of the estimated IF molecular is certainly smaller than large macromolecules such as proteins with molecular weights on the order of kDa, which drastically reduces the possible identities of the molecule.

3

BIOLOGICAL DESCRIPTION OF INHIBITION

Our investigations into the properties of inhibition indicated that it is governed by a diffusible inhibitory factor (IF) which is released by WT cells. We estimated this IF to have a relatively low molecular weight, lower than what would be characteristic of a protein. In this chapter, we explore the biological characteristics of inhibition to form a more complete understanding of the phenomenon. In particular, we investigate the environmental circumstances under which inhibition is effected, what strains and species of bacteria are capable of producing the IF, what the identity of the IF is, and the molecular mechanism governing its effect. The experiments described in this chapter were performed by University of Texas at Austin Department of Molecular Biosciences graduate student Karishma Kaushik, and jointly analyzed by Nalin Ratnayeke and Karishma Kaushik. This work is described in further detail in Kaushik et al. [22]

NOTE: *In this section, when a strain is described as effecting inhibition, this means that when cells of this strain are placed on the disc, zone of inhibition on antibiotic-resistant mutants are formed.*

3.1 INHIBITION IS GOVERNED BY A DIFFUSIBLE MOLECULE

The results of the disc-diffusion assays indicated that inhibition acts at a distance. In order to confirm that this was in fact mediated by a diffusible inhibitory factor, we performed experiments to rule out cell-to-cell contact or proximity mediated inhibition and nutrient depletion. Inhibition mediated by the contact or proximity of cells on the disc to cells on the lawn could be a reasonable explanation for our observations if the deposited cells on the disc moved out and inhibited cells a distance away from the disc. Such forms of inhibition, dependent on contact or close proximity (<< millimeter scales), have been described in previous studies[29, 30]. Similarly if inhibition were due to nutrient depletion by discs on the disc, we would expect this to be translatable over a distance.

3.1.1 *Inhibition is not due to cell-to-cell contact or proximity*

Bacterial inhibition which depends on cell-to-cell contact or proximity, mediated by pathways such as type III secretion systems, has been seen in other similar contexts[29]. To eliminate the possibility of cell-to-cell contact or proximity, we examined a variety of flagellum and pilus loss-of-function mutants (*fliC*, *fliA*, *pilT*) which were deficient in active motility. These mutants were deposited onto the disc instead of WT cells in the disc-diffusion assay. These

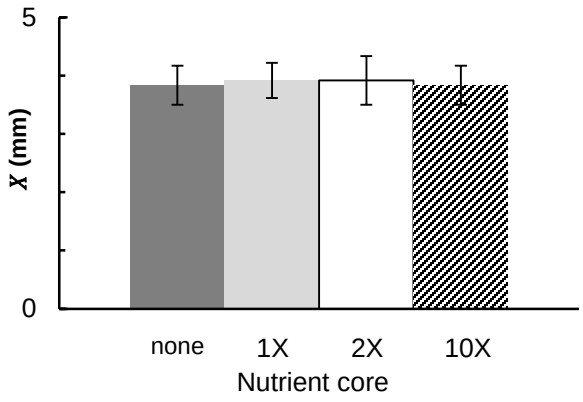

Figure 9: INHIBITION IS NOT DUE TO NUTRIENT DEPLETION. WT PA14 cells were deposited onto LB-tobramcyin 8 μg/mL agar with no cores, and on agar cores containing single (1X), double (2X) and ten-times (10X) nutrient cores. Each core was surrounded by a lawn of resistant mutants on normal antibiotic agar. No significant difference in X was observed (N = 3). Figure adapted from [22].

mutants, while not capable of actively moving outside of the disc, still produced zones of inhibition of comparable size to WT cells. Additionally, we ruled out passive movement from the disc, due to the fact that WT cells when deposited on discs on antibiotic-free plates fail to show show growth very far from the disc (Fig. 11). Thus, cells involved in inhibition must interact through a long-ranged mechanism, such as through diffusion, that is not dependent on physical contact between cells.

3.1.2 *Inhibition is not due to nutrient depletion*

To examine the possibility of nutrient depletion, we observed the impact of modulating the nutrient levels in localized regions (cores) on the agar plate. In these experiments, LB agar cores with 1x, 2x, and 10x nutrient concentrations and 8 μg/mL tobramycin were created in 8 μg/mL tobramycin LB agar plates by cutting out sections from an agar plate and filling them with different agar. Discs with WT cells were then placed on the cores and the assay was performed normally. If nutrient depletion was the mechanism behind inhibition, in which WT cells consumed nutrients at the disc and prevented mutants in the surrounding area to grown into a bacterial lawn, we would expect increasing the nutrient concentration in the cores to decrease zone size. However, no significant change in zone size was observed (Fig. 9).

CORE EXPERIMENT: *A variation of disc-diffusion experiment. Discs are placed on an agar core with different composition than the plate.*

Additionally, we created a nutrient sink agar core, containing antibiotics but no nutrients. Nutrients would diffuse into the core and act similarly to a situation in which cells were consuming nutrients from the surrounding

area. No zone of inhibition was seen around this nutrient-free core. These results show that nutrient levels do not significantly alter inhibition, and that inhibition is not caused by nutrient limitation. This result makes theoretical sense, since WT cells likely die soon after being exposed to the antibiotics.

3.2 PRODUCTION AND ACTION OF THE INHIBITORY FACTOR

Having established that inhibition is governed by a diffusible inhibitory factor, we sought to determine the conditions under which it effects mutant inhibition, and under which it is produced. These properties are not only of intrinsic use to us but also shed light on the factor's identity. To this point, our observations of inhibition had been seen with *P. aeruginosa* WT cells inhibiting *P. aeruginosa* mutant cells in the presence of tobramycin in LB media. Vital questions remained however: 1) what the conditions necessary for the production of IF are, 2) whether antibiotics are required for the action of IF, and 3) whether IF is a specific *P. aeruginosa* product or more generally produced. For these investigations, the disc-diffusion assay was used as an easy indicator for the presence of inhibition under a given set of circumstances, as inhibition zones provide an easily visible and quantifiable readout for inhibition.

3.2.1 *Production conditions for the inhibitory factor*

Two obvious conditions which the production of the inhibitory factor by *P. aeruginosa* cells may depend on are the presence of antibiotics and nutrients. Our previous results in Section 3.1 indicate that the presence of nutrients under the cells do not impact zone size, and we find that increasing the diameter of nutrient-free cores does not alter the inhibition zone size (Fig. 10). This implies that nutrients are not a necessary condition for the production of IF, and indeed, when there are no nutrients available underneath the disc, we still observe IF production.

If the cell stress or death incurred when cells on the disc are exposed to antibiotics triggers the release of the inhibitory factor, we would expect inhibition to be heavily dependent on the presence of antibiotics. When the agar plate does not contain antibiotics, we see no inhibition, even at low initial lawn densities (Fig. 11). However, this could be because IF is not produced without antibiotics, does not act without antibiotics, or both.

To determine which of these scenarios is the case, a similar experiment to that described in the previous section in which a core with a different composition than the surrounding agar was formed in the area below the disc. In this way, the conditions of the cells at the disc and on the agar plate can be decoupled. An agar core was created with the same nutrient composition as the surrounding agar, but without tobramycin. While tobramycin is still free

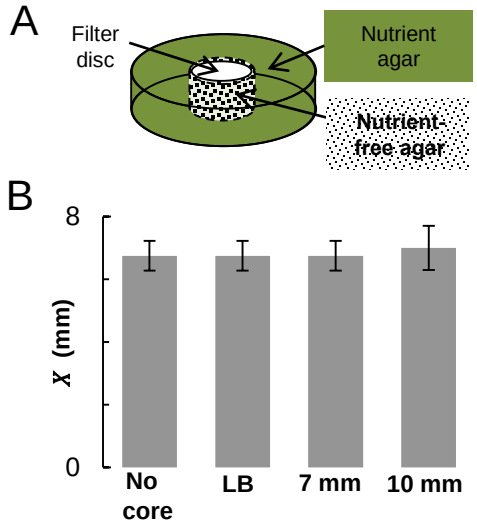

Figure 10: UTILIZATION OF NUTRIENTS ON THE AGAR PLATE IS NOT NECESSARY FOR THE PRODUCTION OF THE IF. A) Schematic of core experiments with nutrient-free agar underneath the disc. B) WT PA14 cells were deposited on discs with no core, and nutrient-free cores of varying diameter. As a control, a core with LB-tobramycin was also used. Each of these was surround by LB-tobramycin 8 μg/mL agar. We find that different core conditions and sizes have no significant impact on the zone size ($N = 4$). Figure adapted from [22].

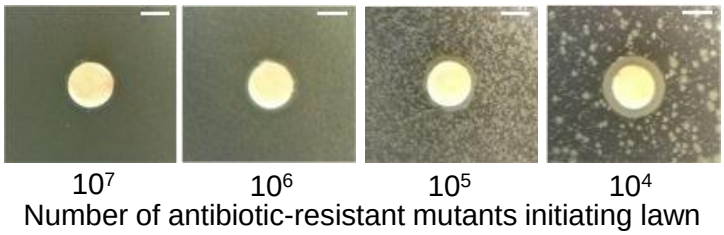

Figure 11: INHIBITION DOES NOT HAPPEN IN THE ABSENCE OF ANTIBIOTIC.WT PA14 cells were deposited on decreasing densities of antibiotic-resistant mutant lawns ($10^7 - 10^4$ cells) on antibiotic-free LB agar. WT cells grow in the region of deposition but do not produce zones of inhibition. Scale bars are 5 mm. Figure adapted from [22].

to diffuse into this core and come in contact with the cells on the disc which is placed on top of it, it would introduce a time lag. Since the characteristic diffusion time for a molecule to diffuse over length l is given by l^2/D, and our estimated value of D for tobramycin is $9.6 \pm 0.8 \times 10^{-7}$ cm^2/s, we would expect the lag to be on the order of tens of hours, which our results in section 2.3 indicate would decrease the inhibition zone size. Additionally, this time lag would increase with increasing core size. We find neither a significant difference in zone size between cells on no core and on an antibiotic-free core, nor a decrease in zone size with increasing core size (Fig. 12). These results indicate that antibiotics are not required for the production of IF.

3.2.2 *Antibiotics are required for the action of the inhibitory factor*

Our finding that inhibition is not seen on plates without tobramycin, combined with our finding that IF is produced regardless of the presence of tobramycin implies that the mutant cells on the lawn only respond to IF when exposed to antibiotics. To further confirm this, we performed the core experiment from the previous section with reversed geometry: the core contained antibiotics and the surrounding plate did not. As expected, we found that no zones of inhibition were formed (Fig. 12).

We find that mutant cells grow better in environments without antibiotics, so the increased growth could lead to smaller zones which are not detectable (Fig. 5). To control for this, we reduced the inoculum size on the plate, and still found no detectable zone size, even when the lawn numbers were low enough to see discrete colonies (Fig. 12). Thus, antibiotics are required for the action of IF, while IF is produced regardless of the presence of antibiotics.

3.2.3 *Inhibition is effected by a large variety of microbes and a second aminoglycoside*

A related question to the production and action conditions of the IF with monocultures of *P. aeruginosa* is whether other strains and species produce the IF as well. We find that the same strain of antibiotic-resistant mutants which we place on the lawn produces inhibition of the mutants on the lawn. This indicates that the mutants are able to inhibit very closely related bacteria (coming from the same progenitor overnight culture), and also implies that there are no significant genetic differences between WT cells and resistant mutant cells when it comes to inhibition. The latter implication is supported by the finding that similar zone sizes are seen for mutant and WT cells on the disc, and that cell stress and/or death due to antibiotics is not necessary for the production of IF. Indeed, we see that strains with MICs orders of magnitude larger than the concentration of tobramycin on the plate still produce inhibition.

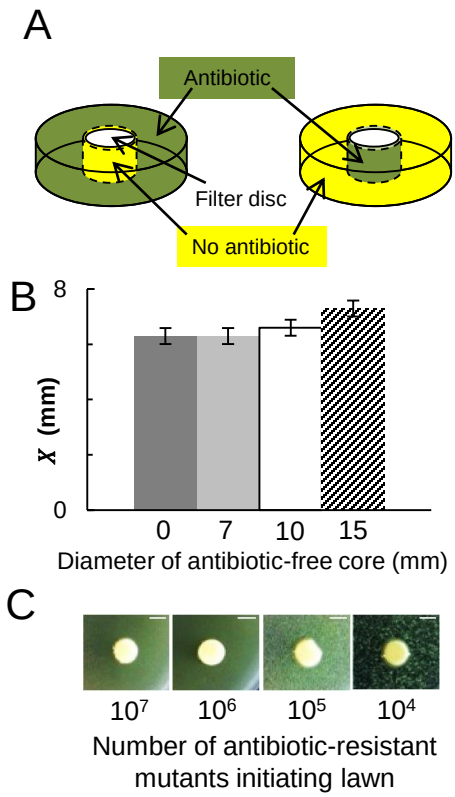

Figure 12: THE INHIBITORY FACTOR IS PRODUCED WITHOUT ANTIBIOTIC, BUT ONLY ACTS IN THE PRESENCE OF ANTIBIOTIC.A set of complementary experiments were performed to determine the role of antibiotics in inhibition. A) Schematic of experiments. Cores of antibiotic-free media and antibiotic-containing media surrounded by antibiotic-containing media and antibiotic-free media respectively were used. B) Antibiotic is not required for production of the IF. WT cells were deposited on agar cores of varying size containing antibiotic-free LB agar, or on no core (0 mm core). We see no significant decrease in zone size between these conditions. B) Antibiotics are required for the action of the IF. WT cells were deposited on cores containing LB-tobramycin agar and surrounded by varying numbers of mutants. No zone of inhibition was seen, even at low initial lawn densities. Scale bars are 5 mm. Figure adapted from [22].

species/strains	additional remarks
Pseudomonas strains	
P. aeruginosa (PA14, PAO1)	Laboratory strains
Clinical *P. aeruginosa* strains	Cystic Fibrosis Isolates
Sandgrass isolate	Uncharacterized environmental isolate
P. fluorescens	Environmental isolate
Other microbial species	
E. coli (DH5α, SM10)	Laboratory strains
S. aureus (Mu50)	Gram-positive, methicillin/vancomycin-resistant clinical isolate, co-pathogen with *P. aeruginosa*
Serratia marcescens	Gram-negative, nosocomial human pathogen
Burkholderia cepacia	Gram-negative, nosocomial co-pathogen with *P. aeruginosa*

Table 1: microbial species/strains which we see produce inhibition Table adapted from [22].

Additionally, we find that the IF is produced by strains of *P. aeruginosa* other than the one primarily used in this study (PA14), as well as other microbial species. We tested a set of microbes which included both Gram-negative and Gram-positive bacteria, some of which are co-pathogens with *P. aeruginosa*, as well as 17 clinical isolates of *P. aeruginosa* all of which produced inhibition (Fig. 13). However, we find that the yeast *Saccharomyces cerevisiae* fails to produce zones of inhibition. The production of the zones of inhibition is consistent with what we find with PA14 (i.e. not produced in the absence of antibiotics), so that we can assume that a similar IF is being produced in all cases. This indicates that the IF is produced by a wide range of bacterial species, but is notably znot produced in sufficient quantities in *S. cerevisiae.*

We also find that inhibition occurs in the presence of another aminoglycoside antibiotic, gentamycin. The antibiotic-resistant mutant which we isolated and used in the previously described experiments had elevated MIC to gentamycin (MIC = 9.7 μg/mL) so that the same experiments and strains used before could be used, and we observe similar results.When these mutants are deposited on the disc, we find that they too produce IF and inhibit mutants

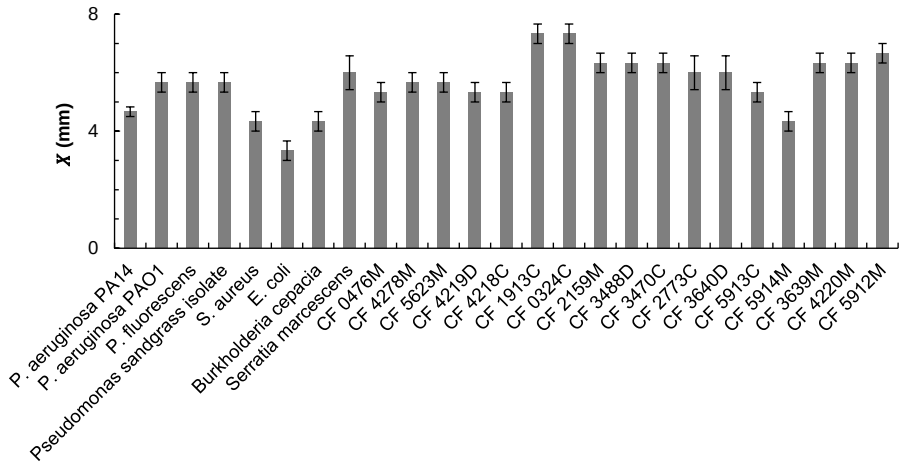

Figure 13: A BROAD RANGE OF BACTERIAL SPECIES AND STRAINS PRODUCE INHIBITION. For each isolate, $10^9 - 10^{10}$ cells were deposited under standard disc-diffusion conditions for inhibition on LB-tobramycin agar. All bacterial species tested produce inhibition, as did all *P. aeruginosa* clinical isolates (CF *). N = 3. Figure adapted from [22].

on the lawn. Interestingly we also find that different mutants with gentamycin resistance cassettes (MIC = 2.5 mg/mL) also produce inhibition. These cells likely do not experience much stress, and certainly don't die to the gentamycin. This is consistent with the finding that antibiotics and resulting cell stress or death is not required for IF production.

Additionally, to confirm that killing by inhibition is not a specific quality of the antibiotic-resistant mutant which we primarily use, we tested the susceptibility of five other antibiotic-resistant mutant strains. Three were produced from spontaneous mutation in antibiotic-free media and isolated in the same was as the previously described mutant, and two were evolved in the presence of tobramycin-containing media. All of these strains exhibit susceptibility to the IF, which indicates that killing by inhibition is not a unique property of our mutant, and is likely a relatively common property of antibiotic-resistant *P. aeruginosa* that isn't dependent on the exact mutations conferring resistance.

3.3 IDENTIFICATION OF THE INHIBITORY FACTOR AND ITS MECHANISM OF ACTION

As described in the previous section, we find that the IF is produced by a wide range of microbial species, and is produced without the presence of antibiotics. This suggests that the IF may be a natively produced metabolic product, rather than a specific inhibitory molecule which targets *P. aeruginosa* mutants. This would explain why *P. aeruginosa* produces this molecule - not so that it can

inhibit its closely related siblings, but rather because it is a naturally produced metabolic product which only is lethal when aminoglycoside antibiotics are in the environment. With this in mind, in this section we investigate the role of metabolism in the production of the IF in order to gain insight into its identity. We also investigate potential mechanisms of action of the IF.

3.3.1 *Core metabolism may be involved in inhibition*

The observation that the yeast *S. cerevisiae* was the only microbe tested which did not produce inhibition suggests that metabolism may be involved the production of the IF. All of the bacterial species tested were grown overnight in LB medium, in which amino acids are the only significant carbon source. Bacteria growing in this medium primarily use amino acid catabolism for their energetic and growth needs. On the other hand, *S. cerevisiae* was cultured in YPD medium, in which dextrose is added to amino acids as a carbon source. Yeast in this medium primarily use fermentation [31]. Thus, differences in the products of carbohydrate metabolism and amino acid metabolism may lead to the observed differences between yeast and bacteria.

In Section 3.2 we found that nutrients on the plate after cells are deposited are not required for the production of IF, which indicates that the metabolism of cells after being placed on the disc does not significantly alter the release of IF to the surrounding area. Additionally, we find that depositing plain LB or YPD media does not produce zones of inhibition. However, molecules created during overnight growth could be released on the plate. While the overnight supernatant was washed from cells, metabolic by-products from the overnight culture could be carried over to the plate intracellularly. Thus, altering the nutrient conditions of the overnight culture could alter whether the IF is produced after cells are placed on the plate.

We cultured *P. aeruginosa*, *E. coli*, *S. aureus* and *S. cerevisiae*. Both *E. coli* and *S. aureus* are capable of either catabolizing amino acids or undergoing sugar fermentation , while *P. aeruginosa* preferentially using amino acids even in the presence of sugars, and *S. cerevisiae* can only ferment. We grew these microbes in either LB, which only contains amino acids, and YPD, which contains both amino acids as well as sugars. We found that when cultured in LB overnight, all three bacterial species produce the IF and produce zones of inhibition. As expected, *S. cerevisiae,* does not grow well in LB, which lacks sugars for fermentation, and does not grow to significant levels. Even when the number of cells of *S. cerevisiae* are the same as those of bacterial discs, we do not see any visible inhibition. This is consistent with the idea that the IF is a product of amino acid catabolism, which *S. cerevisiae* does not significantly use.

When cultured in YPD overnight, *P. aeruginosa* still produces inhibition, while the other three microbes do not (Fig. 14). When cultured in YPD, *S.*

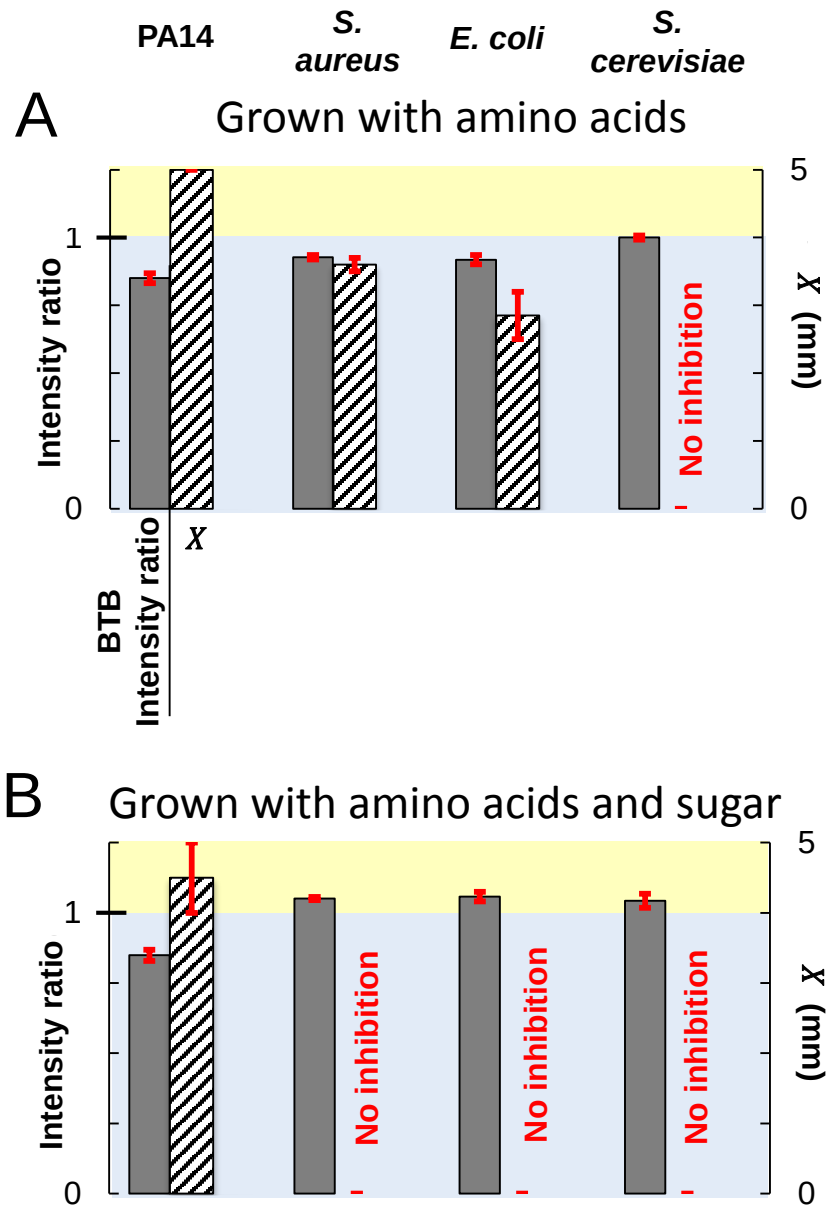

Figure 14: THE CARBON SOURCE USED FOR GROWTH IMPACTS WHETHER THE IF IS PRODUCED. WT PA14, *S. aureus*, *E. coli* and *S. cerevisiae* were grown overnight either in LB (A) or YPD (B) media. LB contains only amino acids as a major carbon source, while YPD has both amino acids and sugar. Following overnight growth, cells were deposited onto LB-tobramycin agar in a standard disc-diffusion test and zones were measured. Additionally, cells were deposited onto discs on LB-tobramcyin BTB agar, and the color change resulting from pH was quantified as described in Fig. 15. An intensity ratio > 1 represents an acidic change, while < 1 represents an alkaline change. A) When grown on amino acids only, the three bacterial species produce zones of inhibition as well as an alkaline color change. B) When grown in the presence of sugars, only *P. aeruginosa*, produces inhibition zones and alkaline color change, while the others produce no inhibition and an acidic change to the medium. Sterile media and overnight culture supernatant produce no inhibition or BTB change. Figure adapted from [22].

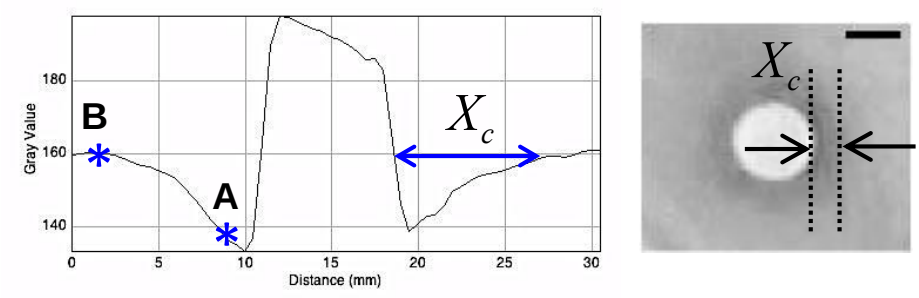

$$\text{Intensity ratio} = \frac{\text{Gray value at point A}}{\text{Gray value at point B}}$$

Figure 15: QUANTIFICATION OF THE WIDTH OF INHIBITION AND INTENSITY RATIO. Using intensity plots generated in ImageJ, intensity ratios were calculated as the gray value at a fixed distance of 2 mm from the disc (A) divided by the gray value at the edge of the alkaline change X_c, which we estimate by eye. For each disc, measurements were taken through perpendicular axes and the average value was used. Scale bar is 5 mm. Figure adapted from [22].

cerevisiae is able to ferment and thus use an alternate metabolic pathway than amino acid catabolism. However, *P. aeruginosa* is not capable fermenting and thus will primarily metabolize amino acids. These two observations are consistent with inhibition being associated with products from amino acid catabolism. However, *E. coli* and *S. aureus*, which are capable of both forms of metabolism, could theoretically use either in YPD. In the next section, we confirm that *E. coli* and *S. aureus* utilize fermentation primarily on YPD, further supporting our hypothesis that amino acid metabolism produces the IF, rather than fermentative metabolism.

3.3.2 *The inhibitory factor may be an alkaline product of amino acid catabolism*

To confirm which form of metabolism is used in different media and species, we observe the pH in the agar area around discs. Amino acid catabolism produces alkaline by-products, and indeed the pH of overnight LB cultures of *P. aeruginosa* is ~ 8. On the other hand, fermentation of sugar products produces acidic by-products, and the pH of overnight YPD *S. cerevisiae* cultures is ~ 6. Supernatant from both overnight LB cultures and YPD cultures of *P. aeruginosa* does not produce inhibition when placed on discs, but we attribute this to a subcritical concentration of the IF in the supernatant.

To examine the pH of molecules released from cells on the discs, we used agar plates which contained bromthymol blue (BTB), a pH indicator with a

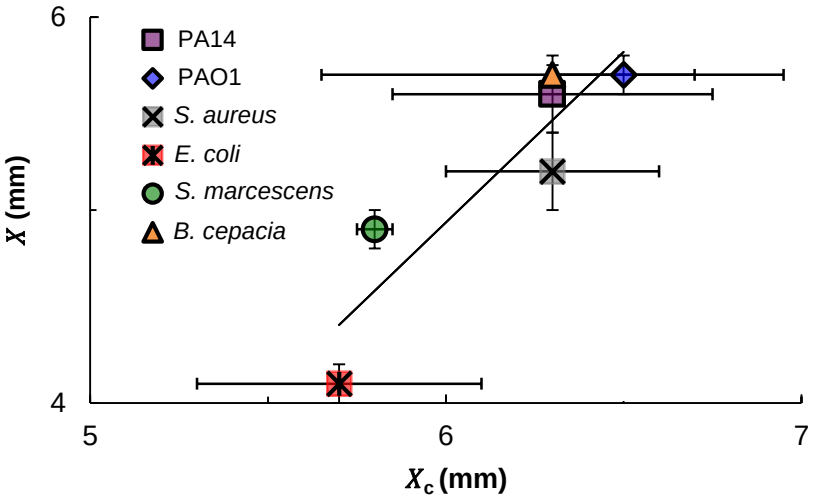

Figure 16: ALKALINE METABOLIC BY-PRODUCTS CORRELATE WITH INHIBITION.For different inhibiting strains, we measured the color change size X_c and inhibition zone size X. We observe a correlation between the two (Pearson's correlation coefficient $r = 0.9$). Intensity profiles were used to measure X_c using image analysis software. For each point, X and X_c represent the average of four measurements along two perpendicular axes. $N = 2$. Figure adapted from [22].

dynamic range of $6 - 7.6$. This indicator is yellow at acidic pH, and blue at alkaline pH. In general, zones of color change could be seen around the discs. To quantify these color changes, color images of plates were taken and split into RGB components. The red channel was analyzed, and the ratio between the intensity 2 mm from the edge of the disc and the value far from the disc were calculated. Intensity ratios < 1 represent a blue color and alkaline pH, while ratios > 1 represent yellow color and acidic change (Fig. 15).

When cultured overnight in LB, we see that all tested bacterial strains released alkaline products out of the disc. Additionally, we find that the size of the inhibition zone (X) and the width of the alkaline color change (X_c) are correlated, which indicates that the IF may be an alkaline product or products of amino acid catabolism (Fig. 16). When cells are placed on discs on nutrient-free agar, we observe similar patterns. This further confirms that nutrients on the plate are not required in order to effect a change in the area around the disc, and that even dying cells are capable of producing a change in the short period of time before they die. *S. cerevisiae* does not produce any color change, which is consistent with the lack of growth in the overnight medium, neither producing significant amounts of alkaline nor acidic products.

As expected, when cultured overnight in YPD, *P. aeruginosa* produces an alkaline color change, indicating it still produces alkaline products even in the

presence of sugars (Fig. 14). This is consistent with the fact that *P. aeruginosa* does not ferment and produce acidic products to significant levels. *S. cerevisiae*, *E. coli* and *S. aureus* however effect an acidic change around the disc, consistent with them utilizing fermentation in the presence of sugars. These results shed light onto our observations that *E. coli* and *S. aureus* do not produce inhibition when cultured overnight in YPD. In YPD, these bacteria preferentially use fermentative metabolism, and thus do not produce the alkaline products of amino acid catabolism that they normally produce in LB. Indeed, the pH of their overnight cultures are acidic. Thus the nutrient conditions of the environment can act as a "switch" which modulates the production of the IF.

Overview of metabolism results

Aggregated, our results indicate that there is a correlation between the production of the IF and the metabolic state of cells. Of the several species of microbes that we investigated, including several *P. aeruginosa* species, *E. coli*, *S. aureus*, and *S. cerevisiae*, we found that all cells that effected inhibition utilized amino acid catabolism in the overnight culture medium and released alkaline products on the agar plate, while all cells that didn't effect inhibition utilized fermentation in the overnight culture and released acidic products. Thus, we conclude that the IF which mediates inhibition is likely either a product of amino acid catabolism, or a molecule which is correlated with it.

3.3.3 *The inhibitory factor is not a reactive oxygen species*

To further rule out other known inhibitory molecules, we ruled out reactive oxygen species as molecular agents of inhibition. Bacteria produce reactive oxygen species (ROS) as a metabolic by-product, and the production of ROS has been implicated in the action of many antibiotics. Biologically relevant ROS include hydrogen peroxide (H_2O_2), superoxide (O_2^-) and hydroxyl radicals (OH^-). To test the role of these products, we eliminated sources of each of these species. We introduced catalase, which breaks down hydrogen peroxide, into the agar medium, and found no significant difference in inhibition zone sizes. As a control, we deposited H_20_2 onto discs alone, which caused zones of inhibition to form, and found that catalase drastically reduced these zone sizes. Additionally, we tested inhibition from a phenazine-null mutant (Δ*phz1/2),* which lacked phenazine operons. Phenazines are associated with the production of all three relevant ROS. We found no significant difference between the zones created by this mutant and the WT. Thus we infer that the IF is not an ROS.

3.3.4 *The inhibitory factor acts through alkaline pH change*

To determine if the alkaline pH change that we observe is correlated with inhibition is causally linked to it, we investigated the effect of exogenous bases on discs, rather than cells. We deposited ammonium hydroxide (NH_4OH), sodium hydroxide (NaOH), and sodium bicarbonate ($NaHCO_3$) onto discs on both BTB-containing LB-tobramycin agar, as well as on agar inoculated with cells. These compounds all produced and alkaline change similar to what we saw in previous experiments, and also produced inhibition of antibiotic-resistant mutants when on LB-tobramycin plates. On antibiotic-free LB agar, the zones of inhibitions are either absent (with NH_4OH and $NaHCO_3$) or significantly reduced (with NaOH), indicating that basic compounds can recreated our observations of inhibition.

Additionally, we deposited 10 µL of varying concentrations of these basic compounds on discs and measured the resulting size of the zones of inhibition. Using linear regression to determine the relationship between concentration and X , we estimate that 10 µL of 2.04M NH_4OH, 1M NaOH, or 1M $NaHCO_3$ produces inhibition zones which are comparable to those seen with cells ($x = 5$mm) (Fig. 17). Similarly to what we see with cells, we see a correlation between the size of the color change and the zone of inhibition caused by exogenous bases (Fig. 18).

Others have shown that alkaline pH changes can significantly enhance the bactericidal activity of aminoglycosides (i.e. decrease MIC) [32, 33]. At least two mechanisms for this pH-dependence of aminoglycoside activity have been suggested: 1) an increased proton motive force which increases the uptake of the antibiotics [33–35]; 2) an increased proportion of aminoglycoside molecules found in their non-ionized, more-bactericidal form [33]. As a result, we infer that the IF inhibits antibiotic-resistant mutants by increasing pH, which increases the activity of the antibiotics in the medium.

3.3.5 *Biogenic amines are plausible candidates for the inhibitory factor*

A wide range of microbes produce basic compounds such as ammonia and other amines as by-products of amino acid catabolism. Ammonia is a low molecular weight molecule (MW = 17 Da), which is consistent with our estimate of the IF molecular weight. Ammonia production from bacteria has been shown to mediate long-range intercellular interactions, as well as influence antibiotic resistance. Recently, gaseous ammonia released from bacterial culture supernatant, and trimethylamine was shown to decrease resistance to the aminoglycoside antibiotics kanamycin and spectinomycin[36].

We used an ion-selective electrode to measure ammonia and amine emission from deposited bacteria and yeast. We find that *P. aeruginosa* emits nearly

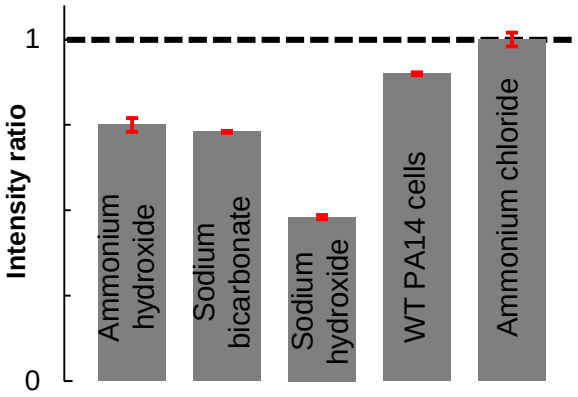

(a) Exogenous compound intensity ratios

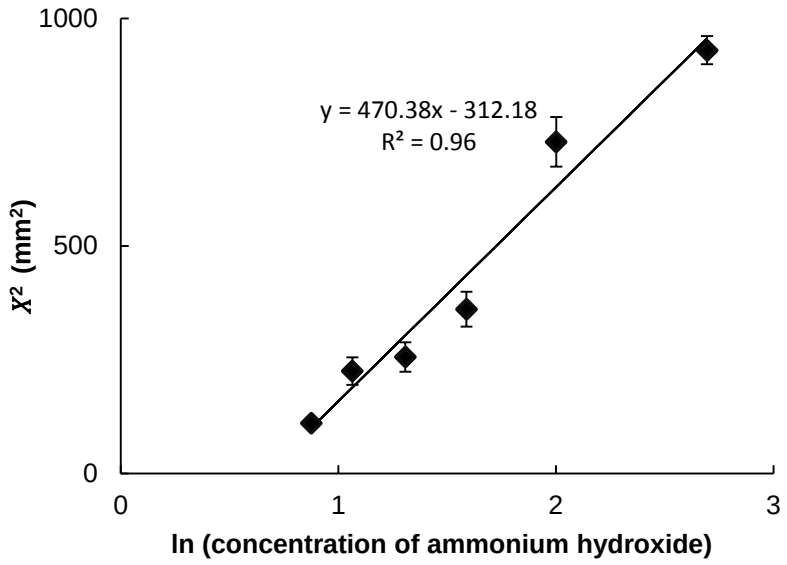

(b) NH_4OH concentration changes zone size

Figure 17: EXOGENOUS ALKALINE SOLUTIONS CAN RECAPITULATE INHIBITION. a) 10 µL of exogenous compounds (2.4M NH_4OH, 1M $NaHCO_3$, 1M NaOH, WT PA14 cells, and 1M NH_4Cl) were deposited on LB-tobramycin BTB agar and intensity ratios were measured. The three bases and WT cells all produced an alkaline change, while NH_4Cl produced an approximately no change change. b) Varying concentrations of NH_4OH were deposited onto discs. A linear relationship between X^2 and the log of the concentration is seen, similar to antibiotics ($R^2 = 0.96$). Figures adapted from [22].

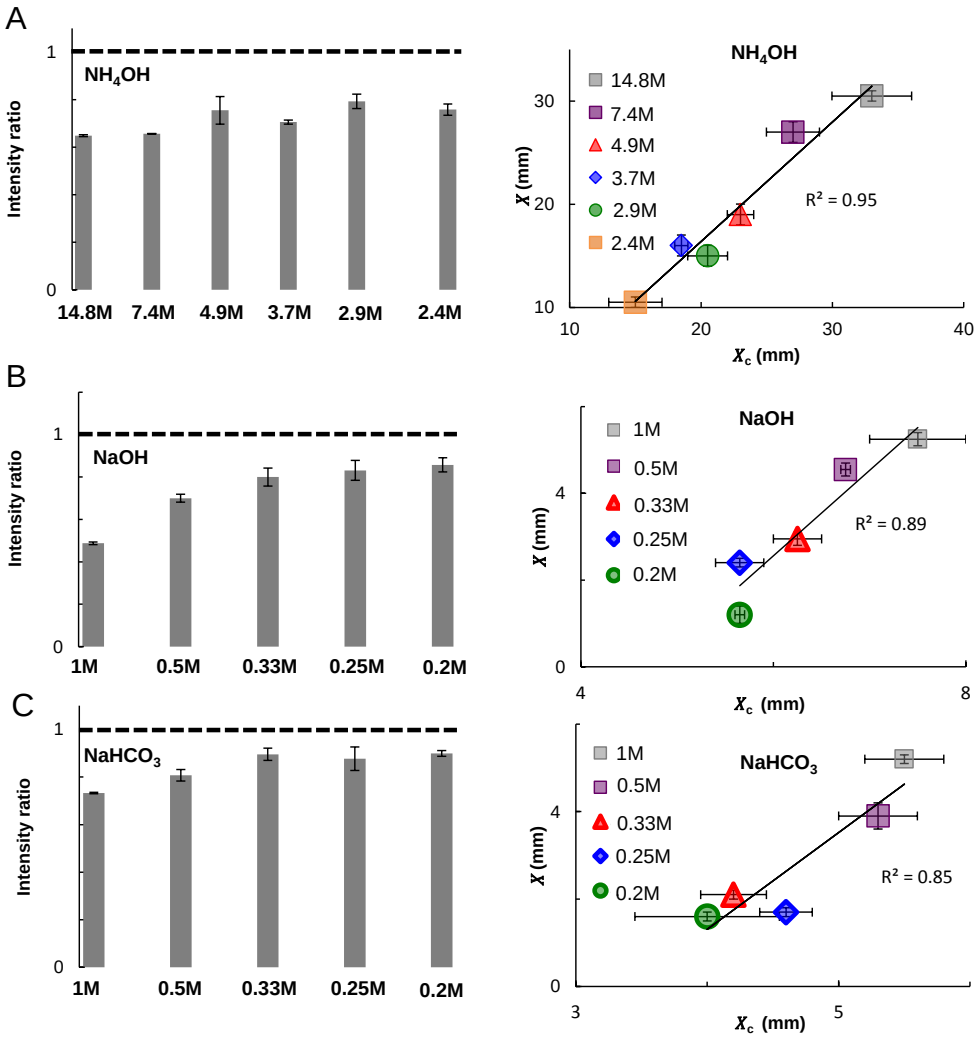

Figure 18: ALKALINE CHANGE PRODUCED BY EXOGENOUS BASES CORRELATES WITH INHIBITION. 10 µL of decreasing molar concentrations of exogenous alkaline compounds (A) NH_4OH, (B) NaOH and (C) $NaHCO_3$ were deposited on LB-tobramycin BTB agar and on antibiotic-resistant lawns overlaid on LB-tobramycin agar. Intensity ratios and the color change zone size X_c was calculated as described in Figure 15. Each compound had a roughly increasing intensity ratio with decreasing concentration, as expected, and we see that there is a correlation between X_c and X. Figure adapted from [22].

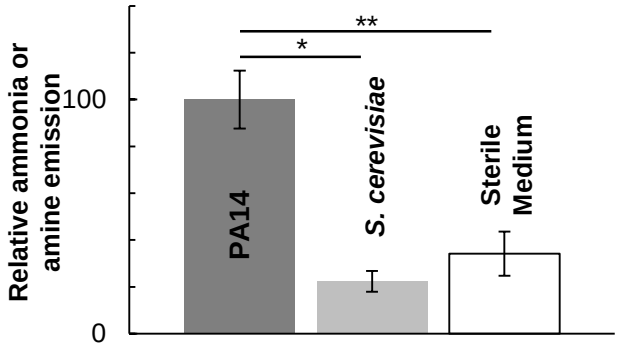

Figure 19: PRODUCTION OF AMMONIA OR AMINES IS ASSOCIATED WITH INHIBITION. Using an ion-selective electrode, ammonia and amine emission was measured following deposition of WT PA14 and *S. cerevisiae* cells on discs on LB-tobramycin in vials. Emissions were normalized to the PA14 average. Significantly higher amounts of ammonia were detected from PA14 than *S. cerevisiae*. N = 3. P < 0.005 by two-tailed Student t test. ** P < 0.02 by two-tailed Student t test. Figure adapted from [22].

five times the ammonia and amine levels as *S. cerevisiae*, a microbe which does not produce inhibition. We additionally find that, in the disc diffusion assay, deposition of ammonium chloride (NH_4Cl) at similar concentrations to the other exogenous compounds produces a slightly acidic change and fails to produce inhibition (Fig. 19). Thus we find a correlation between alkaline pH change and inhibition, but no significant effect from the specific properties of the ammonia molecule when not in alkaline environments. This either means that ammonia must be in its unionized form in order to effect inhibition, or that the increase in pH following its release is the proximate cause of cell death. In light of the results from the previous section however, the latter is more likely.

Therefore, we tentatively identify the IF as biogenic ammonia and/or other low molecular weight amines which effect an alkaline pH change which in turn causes antibiotic-resistant mutant cells to die in the presence of aminoglycosides. The production of amines can be attributed to amino acid catabolism, which is modulated by the nutrient conditions of the environment.

Part III

MODELING

4

MODELING INHIBITION

Informed by the physical and biological properties of inhibition which we uncovered in the previous chapters, we sought to further model its behavior. There are a couple findings in particular which motivate these models. First, the observation that the mechanism of action of the IF could involve pH led us to examine what effect it could have on the model developed in Section 2.2. Secondly, we find that in the spatially-mixed system survival probability approaches zero with increasing cell density (Fig. 2b). However mutant cells are able to grow into high-density colonies without inhibiting themselves. To resolve this paradox, we examined the effect of small-scale spatial fluctuations in the initial population density, as well as pH-dependent antibiotic resistance in a stochastic physics-based model.

4.1 PH-MEDIATED INHIBITION IN DISC-DIFFUSION ASSAY

In Section 2.2, we describe a model which predicted the molecular weight of the inhibitory factor in the disc-diffusion assay. This model examined the evolution of the IF concentration gradient over time, and took the point at which the concentration was a critical value at the critical time to be the edge of the zone. Our results from Chapter 3 however, indicate that pH rather than the IF concentration may be the immediate cause of death of cells. Since the pH at a given point on the plate should be a monotonic function of the IF concentration, we can modify the disc-diffusion model to incorporate a threshold pH, rather than threshold IF concentration.

It has been shown in several cases that the MIC of aminoglycoside antibiotics decreases exponentially with increasing pH [37]. For an alkaline IF, the concentration of OH^- is approximately of the form

$$[OH^-] \approx A \times [IF]^{\beta} \tag{12}$$

Thus,

$$pH = \alpha + \beta \log_{10}[IF] \tag{13}$$

, where $\alpha = 14 + \log_{10} A$. Combining this with Equation 2 we get:

$$pH = \alpha + \beta \log_{10} \left\{ \frac{[IF]_0}{4\pi Dt} \exp\left(-\frac{x^2}{4Dt}\right) \right\} \tag{14}$$

This can be rearranged to:

$$x^2 = 4Dt \ln[IF]_0 - 4Dt \ln(4\pi Dt) - \frac{4Dt \ln(10)}{\beta}(pH - \alpha) \tag{15}$$

Just as in the previous model, we assume $[IF]_0 = k_0 \times N_0$, where k_0 is a production constant and $N_0$is the number of cells on the disc, and Equation 15 becomes

$$x^2 = 4Dt\ln(N_0) + 4Dt\ln\left(\frac{k_0}{4\pi Dt}\right) - \frac{4Dt\ln(10)}{\beta}(pH - \alpha) \tag{16}$$

This expression gives the point in space x at which the pH is a given value at a given time. If pH modulates the antibiotic resistance of mutants, a critical value of pH, pH_c , should bring the MIC of the mutant below the concentration of antibiotics on the plate. If the zone is formed at the critical time, as assumed in the previous model, the edge of the zone X will satisfy:

$$X^2 = 4DT_c\ln(N_0) + F(D, T_c, pH_c, k_0, \alpha) \tag{17}$$

This expression has a dependence on $\ln(N_0)$ which is of the same form as the one found in the previous model without pH-mediated inhibition (Eq. 5). Thus, pH-mediated inhibition does not alter our estimation of the molecular weight of the the IF.

4.1.1 *pH-mediated inhibition predicts a linear relationship between squared sizes of indicator color change and inhibition zone*

We observe that cells which produce inhibition also cause a zone of color change in agar containing BTB. The perceived edge of this discoloration should correspond approximately to a specific threshold pH, $pH_{c,BTB}$. Similarly, based on alterations to the disc-diffusion model which incorporates pH change, we expect the edge of the zone of inhibition to correspond to another threshold pH, $pH_{c,IF}$ if the IF is mediated by pH change. Therefore from Equation 15, the inhibition zone size X_{IF} is shown by

$$X_{IF}^2 = 4DT_c\ln(N_0) + 4DT_c\ln\left(\frac{k_0}{4\pi DT_c}\right) - \frac{4DT_c\ln(10)}{\beta}(pH_{c,IF} - \alpha) \tag{18}$$

while at the critical time the size of the zone of discoloration X_{BTB} is

$$X_{BTB}^2 = 4DT_c\ln(N_0) + 4DT_c\ln\left(\frac{k_0}{4\pi DT_c}\right) - \frac{4DT_c\ln(10)}{\beta}(pH_{c,BTB} - \alpha) \tag{19}$$

Since the IF is both creating a zone of inhibition, as well as the zone of discoloration, all constants in these equations should be the same value. Thus:

$$X_{IF}^2 = X_{BTB}^2 - \frac{4DT_c\ln(10)}{\beta}(pH_{c,IF} - pH_{c,BTB}) \tag{20}$$

This model therefore predicts a linear relationship between X_{IF}^2 and X_{BTB}^2, when $X_{BTB}$is measured around the critical time. This is consistent with our

observations of a correlation between the two zone sizes (Fig. 16). Additionally, we can infer from these data that the threshold pH value for inhibition is higher than the threshold pH value for the BTB color change. Since the dynamic range of BTB is approximately $6 - 7.6$, the defining of the edge of the discoloration will likely be ~ 7.6. Thus, the threshold value for inhibition should be higher than 7.6.

4.2 INHIBITION IN SPATIALLY-MIXED POPULATIONS

In the spatially-mixed system described in Section 1.3, where varying densities of cells are plated in an agar overlay on an antibiotic-containing plate, we observe that the survival probability of antibiotic-resistant mutants approaches zero with increasing cell density. Similarly, in the disc-diffusion assays, we see that increasing the deposited number of cells at the disc increases the range at which mutants are inhibited. As a result, it seems paradoxical that mutant cells are able to grow into high-density colonies on the plate at all without inhibiting themselves. We see that mutant cells still produce the IF in disc-diffusion assays, indicating this is a relevant question. Additionally, since the mutants we observe are inhibited on the lawn of the disc diffusion assays were isolated from colonies growing on antibiotic containing plates, we infer that a genetic resilience to the IF is not required for a mutant colony to grow. This also begs the question of why certain mutant cells to survive to grow into a colony, while others die. To resolve these questions, we examine the effect of spatial fluctuations in cell density on the survival of antibiotic-resistant mutants.

It has been suggested that the molar quantity of an inhibitory substance *per cell* is a more accurate determinant of cell survival during exposure than the concentrations [13]. This is clearly seen in the inoculum effect, in which higher density populations of bacteria exhibit a higher resilience to antibiotics than those at lower densities [12, 13]. According to this interpretation, in a well-mixed, homogeneous environment with a constant antibiotic concentration $[AB]$, increasing cell density decreases the moles of antibiotic per cell, $\{AB\}$, thus increasing the resistance of cells to the antibiotic at a given $[AB]$. However, our results in Section 3.3 have shown that an IF released by cells may decrease antibiotic resistance by increasing the pH of the medium. These two antagonistic phenomena, together with random fluctuations in local cell density lead to non-trivial cell survival rates as a function of average cell density.

4.2.1 *Model derivation*

Dividing molar quantities of antibiotics by a number of cells represents a screening or local alteration of absorption kinetics of antibiotics by cells. This process likely does not occur over long distances. Therefore, we can consider a small effective volume $V_e$in the spatially-mixed system containing N cells. This assumption comes from intrinsic length scales set by biochemical kinetics and diffusion. A reduction in the molar quantity of IF per cell is likely to be dependent only on the cell density in the region surrounding a given mutant cell (mutant cells will not be protected from the IF by cells far away from them). However, the diffusion of the IF over large distances implies that the concentration profile of the IF likely is not constrained by this volume. Thus, we can assume a uniform $[AB]$ throughout the plate, and the resulting$\{AB\}$ in the effective volume is accordingly given by $\frac{[AB]V_e}{N}$. If $\{AB\}$ is less than a threshold value $\{AB\}_c$, we expect mutant cells in V_e to grow. Since there are orders of magnitude more WT cells than mutant cells and the effective volume is small, we expect there to be no more than one mutant in a given V_e together with WT cells. Therefore, the survival condition for a mutant is given by

$$N_{WT} + 1 > \frac{[AB]V_e}{\{AB\}_c} \tag{21}$$

, where N_{WT} is the number of WT cells in the volume. The random deposition of bacteria into an agar overlay can be modeled as a Poisson process. Thus, the probability that the number of WT cells in the volume will be greater than N_{WT} is given by

$$P = 1 - e^{-V_e \rho_{WT}} \sum_{i=0}^{N_{WT}} \frac{(V_e \rho_{WT})^i}{i!} \tag{22}$$

where ρ_{WT} is the average density of WT cells on the plate. Since $\rho_{WT} \approx \rho_0$ where ρ_0 is the average total cell density initially on the plate, this probability is approximately described by

$$P = 1 - e^{-V_e \rho_0} \sum_{i=0}^{N_{WT}} \frac{(V_e \rho_0)^i}{i!} \tag{23}$$

Previous studies have found an approximately exponential relationship between pH and MIC to aminoglycosides [37]. Since these studies were performed at uniform cell density, we can also assume that pH and $\{AB\}_c$ also have an exponential relationship, which we can represent as:

$$\{AB\}_c = A \times 10^{-b \times pH} + \{AB\}_{min} \tag{24}$$

where A and b are scaling constants and $\{AB\}_{min}$ is the minimum value of $\{AB\}_c$. As derived in Section 4.1, we can approximate the pH resulting from a given concentration of IF, [IF] as

$$pH = \alpha + \beta \log_{10}[IF] \tag{25}$$

where α and β are constants which account for the acid-base properties of the IF. Assuming $\{AB\}_{min}$ is small compared to $\{AB\}_c$, the condition for mutant survival (Eq. 21) can be rewritten as

$$N_{WT} > \frac{[AB][IF]^{b\beta} V_e}{A \times 10^{-\alpha b}} - 1 \tag{26}$$

Since the IF is distributed throughout the plate and has a relatively high diffusion coefficient (450 ± 50 $\mu m^2/s$), we can assume that [IF] is uniformly distributed. If $[IF] = k_p \rho_0$, where k_p is a production constant, Equations 23 and 26 can be rewritten as the probability of mutant survival:

$$P = 1 - e^{-V_e \rho_0} \sum_{i=0}^{\Gamma V_e \rho_0^{\eta} - 1} \frac{(V_e \rho_0)^i}{i!} \tag{27}$$

where $\Gamma = \frac{[AB] k_p^{b\beta}}{A \times 10^{-\alpha b}}$ and $\eta = b\beta$. Γ is a lumped parameter which accounts for the alkalinity of the IF, and a strain's production of IF and degree of antibiotic resistance; η accounts for the sensitivity of the level of antibiotic resistance to changes in pH; V_e accounts for the spatial extent over which cells surrounding a mutant can lower the $\{AB\}$ to which a mutant is exposed.

The function P (Eq. 27) is discrete with respect to ρ_0, and is defined for densities in which $\Gamma V_e \rho_0^{\eta} - 1$ is an integer (i.e. ρ_0 must be equal to $\left(\frac{n+1}{\Gamma V_e}\right)^{\frac{1}{\eta}}$, where n is a positive integer). However we can approximate a continuous extension of it using linear interpolation. The resulting function $\tilde{P}$ describes the proportion of plated antibiotic-resistant mutants that survive and grow to form colonies on the plate, and is a function of the initial density on the plate. The fraction of the total cells which are plated that grown into colonies M is thus described by $M = \mu \tilde{P}$ where μ is the true proportion of mutants in the population. Similarly, the number of colonies formed C is given by $C = \mu \rho_0 V_{tot} \tilde{P}$, where V_{tot} is the total volume into which the cells are initially embedded.

4.2.2 *Fitting model of spatially-mixed system to experimental results*

When we fit this model to our experimental data, we found that a wide range of values of Γ, V_e, η and μ result in trends which are consistent with our measurements in Figure 2. We can estimate physically reasonable values for

the size of V_e by examining how an individual might impact its surrounding antibiotic concentration in a diffusive system. $V_e$is the effective volume within which cells reduce the amount of antibiotics acting on a cell at its center. The distance at which a cell no longer effects a significant reduction in antibiotic quantities would be equal to the radius of a spherical V_e. To estimate this distance, we model cells as antibiotic sinks.

The diffusion of antibiotics molecules can be described by Fick's Second Law:

$$\frac{\partial[AB]}{\partial t} = D\nabla^2[AB] \tag{28}$$

where $[AB]$ is the antibiotic concentration at a given point. The diffusion of antibiotics is fast relative to the size of a cell (tobramycin diffusion coefficient = 96 ± 8 $\mu m^2/s$), we can consider the steady state distribution of antibiotics around the cell. Approximating a cell to be spherical, the steady state distribution around a cell which completely absorbs antibiotics (i.e. $[AB] = 0$ at the cell surface) is given by

$$[AB] = [AB]_0 \left(1 - \frac{a}{r}\right) \tag{29}$$

where $[AB]_0$ is the antibiotic concentration far from cells, and a is the radius of a cell. Deviations from this due to cells being non-spherical will be small when relatively far from the cell. The concentration at $10a$ away from the cell will be 90% of $[AB]_0$. This corresponds to a volume 1000 times the volume of a cell, and we take this value to be a reasonable minimum bound for V_e. We estimate the volume of a *P. aeruginosa* cell to be approximately 4×10^{-6}nL, which leads to a minimum value of $V_e$of .004 nL.

With a V_e of .004 nL, values of η ranging from .90 to 2.5, Γ ranging from 8×10^{-6} to 4 $nL^{\eta-1}$and μ ranging from 4×10^{-7} to 4×10^{-6}, produce reasonable fits to our data, and the least squares fit has an an η of 1.186, Γ of 0.307 $nL^{\eta-1}$ and μ of 1.02×10^{-6} ($R^2 = .923$). Additionally, a V_e of .04, .4 and 4 nL produce similar trends and fits. Overall, the wide range of parameters which produce reasonable fits to our data reflects a robustness of this model to changes in specific values, and indicates that fine tuning of parameters is not necessary to match the trends which we observe.

4.2.3 *Summary of model results*

Guided by this model, we postulate that antibiotic-resistant mutants are able to grow into high-density colonies because they are shielded from antibiotics by their WT neighbors. A mutant will grow into a colony if it is in a region of high local cell density that reduces the$\{AB\}$ locally below a threshold value. As the average cell density increases, however, the resulting increase in $[IF]$ on the plate lowers this threshold value by causing an increase in pH. These antagonistic processes can result in a net decrease in mutant survival probability

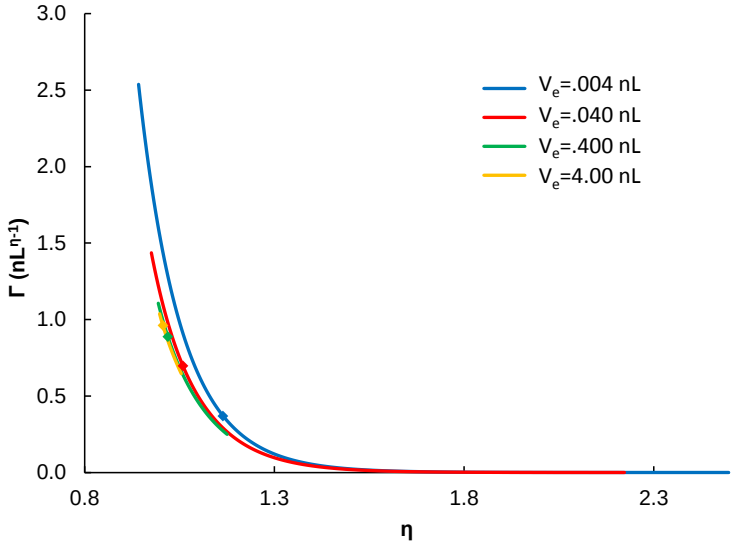

Figure 20: A WIDE RANGE OF MIXED-SYSTEM MODEL PARAMETERS PRODUCE REASONABLE FITS TO OBSERVATIONS. Least squares estimates of Γ and μ, as well as the sum of squared residuals (SSR), were calculated for set values of V_e and η, based on the colony counts from Replicate 1 of Figure 2. A SSR of $1.0 \times 10^6$was considered the threshold for reasonable fits, and fits with a SSR greater than this are excluded. Plotted are the least squares estimated Γ as a function of the set values of η for V_e of .004, .04, .4 and 4. Diamond points (♦) represent the fit values of Γ and η with minimum SSR. Figure adapted from [22].

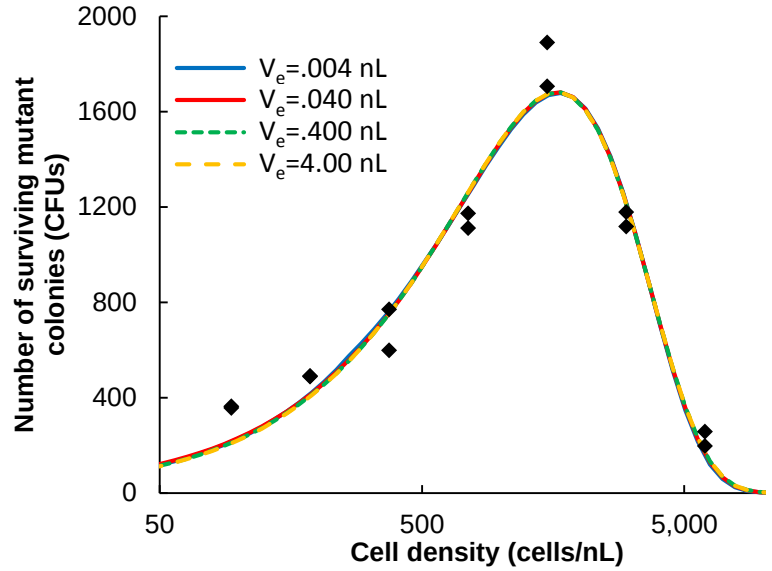

(a) Mutant survival number fits

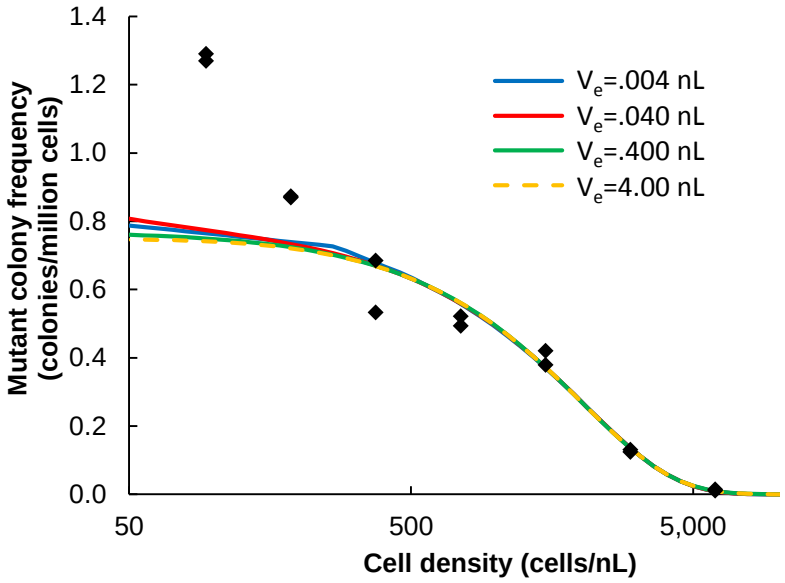

(b) Mutant colony frequency fits

Figure 21: FITS OF THE MIXED-SYSTEM MODEL DESCRIBE OUR OBSERVATIONS WELL. Least squares regression was performed on colony count data from Replicate 1 of Figure __ for given values of V_e. The resulting fit parameters were 1) $V_e = 0.004$, $\eta = 1.164$, $\Gamma = 0.370$, $\mu = 1.10 \times 10^{-6}$; 2) $V_e = 0.04$,$\eta = 1.059$,$\Gamma = 0.697$, $\mu = 1.21 \times 10^{-6}$; 3) $V_e = 0.4$, $\eta = 1.019$, $\Gamma = 0.888$, $\mu = 1.26 \times 10^{-6}$; 4) $V_e = 4$, $\eta = 1.006$, $\Gamma = 0.962$, $\mu = 1.27 \times 10^{-6}$. a) Colony counts fits. $R^2 = 0.953$ ($V_e = 0.004$),0.955 ($V_e = 0.04$), 0.954 ($V_e = 0.4$), 0.954 ($V_e = 4$). a) Mutant colony frequency fits. $R^2 = 0.778$ ($V_e = 0.004$), 0.784 ($V_e = 0.04$), 0.766($V_e = 0.4$), 0.759 ($V_e = 4$). Figure adapted from [22].

with increasing average cell density. This interpretation indicates that the spatial organization of bacteria, as well as their density, influences their growth under these conditions. These interactions depend heavily on the ranges of action inherent to the process, and leads to non-trivial phenomena depending on the spatial distribution of cells. These results also imply that small initial fluctuations in density will be magnified, as they can be prime determinants of the initial survival of bacteria.

CONCLUSIONS

We find that microbial population structure, including cell density, spatial distribution and interspecies interactions, can drastically impact survival of antibiotic-resistant mutants in that population when exposed to aminoglycoside antibiotics. We see that increasing cell density has both positive, and negative effects on survival, and that the net effect is determined in a density and antibiotic concentration-dependent way. Further, we characterize the negative effect, which we term inhibition, and find that the causative agent of this phenomenon is an alkaline by-product of amino acid catabolism. The mechanism of action of this molecule likely is through an effected increase in pH which enhances the bactericidal effect of aminoglycoside antibiotics. Finally, through a probabilistic model, we find that the interaction of intrinsic length scales imposed by the inhibitory molecule and random fluctuations in cell density in homogeneous environments can lead to non-trivial responses of mutant survival to changes in cell density.

Our finding that increasing bacterial density can increase antibiotic susceptibility of antibiotic-resistant mutants is superficially in contrast to previous observations that in dense bacterial populations, such as in biofilms, the susceptibility against antibiotics is in fact decreased. However, it is important to note that bacteria in biofilms are in a different phenotypic state than that of both planktonic cells, as well as the cells which we imbedded into agar. Most notably, biofilms are structured by embedding extracellular polymers, which can provide protection against aminoglycoside antibiotics. The bacteria in biofilm interiors also have limited access to nutrients, which can result in slowed growth and switches to alternate metabolic states that can protect against antibiotics. Thus, both the structure and the phenotypic state of the bacterial population needs to be considered when designing treatment strategies. Our results likely are applicable to the case of initial biofilm formation, as well as the colonization of new environments, which have cell densities that correspond to the densities under which we performed our experiments.

The potential applicability of our results can easily be seen in the case of Cystic Fibrosis (CF) . The CF lung contains an abundance of free amino acids [38–40]. In microbes sampled from CF lungs, the genes and pathways involved in amino acid catabolism are significantly upregulated [38, 39]. In accordance, elevated ammonia levels have been found in CF sputum [32]. These observations would seem to suggest that the microbial population in the CF lung is well-poised to inhibit each other in the presence of aerosolized tobramycin, which is commonly used in the treatment of CF.

However, CF results from a genetic defect in the Cystic Fibrosis transmembrane receptor (CFTR), which causes decreased bicarbonate ion transport and acidification of CF airway fluids [20, 21]. This would prevent inhibition. Inhaled bicarbonate therapy is a possible remediation for this and is already being studied as a therapy for CF because it may help restore the innate antimicrobial activity of airway surface fluids as well as facilitate the thinning and clearing of airway mucus [20, 21]. Our results suggest a potential additional benefit for bicarbonate therapy in CF, where it could augment the activity of aminoglycosides and help curtail antibiotic resistance. Additioanlly, altering the metabolic state of cells in these environments could further impact the environmental conditions of the lung in infected locations alone, and could provide an avenue for targeted treatment of the lung which does not alter the state of the lung as a whole.

Our findings indicate that manipulating the nutritional and metabolic environment of the CF lung, chronic wounds, or other sites of infection could provide a set of management strategies that are complementary to and synergistic with conventional antibacterial therapies. Strategies such as limiting the availability of sugars and using preliminary anti-fungal therapy would promote amino acid catabolism and prevent microbe-caused acidification, facilitating the synergistic interactions of alkaline pH and aminoglycosides. Because the inhibition we characterize here is the result of a product(s) of highly-conserved native bacterial metabolic pathways, at least one avenue of evolutionary escape is likely to be blocked. This is important, given the increasing antimicrobial resistance and the paucity of newer antibiotics. In addition, because the IF is produced by bacteria and will therefore be localized near infection sites, approaches to treatment that exploit the structure of microbial populations may reduce the disadvantages associated with system-wide high concentrations of antibiotics and resultant toxicity to patients. This approach could both help to combat the rise of antibiotic-resistant strains and extend the lifetime of currently available antibiotics.

BIBLIOGRAPHY

[1] Rebecca R Roberts, Bala Hota, Ibrar Ahmad, R Douglas Scott, Susan D Foster, Fauzia Abbasi, Shari Schabowski, Linda M Kampe, Ginevra G Ciavarella, Mark Supino, et al. Hospital and societal costs of antimicrobial-resistant infections in a chicago teaching hospital: implications for antibiotic stewardship. *Clin. Infect. Dis.*, 49(8):1175–1184, 2009. (Cited on page 1.)

[2] James J Foti, Babho Devadoss, Jonathan A Winkler, James J Collins, and Graham C Walker. Oxidation of the guanine nucleotide pool underlies cell death by bactericidal antibiotics. *Science*, 336(6079):315–319, 2012. (Cited on page 1.)

[3] Peter Davey, Jacqueline Sneddon, and Dilip Nathwani. Overview of strategies for overcoming the challenge of antimicrobial resistance. *Expert review of clinical pharmacology*, 3(5):667–686, 2010.

[4] Keith Poole. Overcoming multidrug resistance in gram-negative bacteria. *Curr. Opin. Investig. Drugs*, 4(2):128–139, 2003. (Cited on page 1.)

[5] Qiucen Zhang, Guillaume Lambert, David Liao, Hyunsung Kim, Kristelle Robin, Chih-kuan Tung, Nader Pourmand, and Robert H Austin. Acceleration of emergence of bacterial antibiotic resistance in connected microenvironments. *Science*, 333(6050):1764–1767, 2011. (Cited on page 1.)

[6] Gabriel G Perron, Andrew Gonzalez, and Angus Buckling. Source–sink dynamics shape the evolution of antibiotic resistance and its pleiotropic fitness cost. *Proceedings of the Royal Society B: Biological Sciences*, 274(1623):2351–2356, 2007.

[7] Rutger Hermsen and Terence Hwa. Sources and sinks: a stochastic model of evolution in heterogeneous environments. *Phys. Rev. Lett.*, 105(24):248104, 2010. (Cited on page 11.)

[8] Rutger Hermsen, J Barrett Deris, and Terence Hwa. On the rapidity of antibiotic resistance evolution facilitated by a concentration gradient. *Proceedings of the National Academy of Sciences*, 109(27):10775–10780, 2012.

[9] Bartłomiej Waclaw, Rosalind J Allen, and Martin R Evans. Dynamical phase transition in a model for evolution with migration. *Phys. Rev. Lett.*, 105(26):268101, 2010.

[10] Philip Greulich, Bartłomiej Waclaw, and Rosalind J Allen. Mutational pathway determines whether drug gradients accelerate evolution of drug-resistant cells. *Phys. Rev. Lett.*, 109(8):088101, 2012. (Cited on page 1.)

[11] Kelvin Li, Monika Bihan, Shibu Yooseph, and Barbara A Methe. Analyses of the microbial diversity across the human microbiome. *PloS one*, 7(6):e32118, 2012. (Cited on page 1.)

[12] Robert Eng, Sharon Smith, and Charles Cherubin. Inoculum effect of new beta-lactam antibiotics on pseudomonas aeruginosa. *Antimicrob. Agents Chemother.*, 26(1):42–47, 1984. (Cited on pages 1, 8, and 45.)

[13] Klas I Udekwu, Nicholas Parrish, Peter Ankomah, Fernando Baquero, and Bruce R Levin. Functional relationship between bacterial cell density and the efficacy of antibiotics. *J. Antimicrob. Chemother.*, 2009. (Cited on pages 8 and 45.)

[14] Jodi L Connell, Eric T Ritschdorff, Marvin Whiteley, and Jason B Shear. 3d printing of microscopic bacterial communities. *Proceedings of the National Academy of Sciences*, 110(46):18380–18385, 2013. (Cited on page 1.)

[15] J William Costerton, Zbigniew Lewandowski, Douglas E Caldwell, Darren R Korber, and Hilary M Lappin-Scott. Microbial biofilms. *Annual Reviews in Microbiology*, 49(1):711–745, 1995. (Cited on pages 1 and 7.)

[16] Holly K Huse, Taejoon Kwon, James EA Zlosnik, David P Speert, Edward M Marcotte, and Marvin Whiteley. Parallel evolution in pseudomonas aeruginosa over 39,000 generations in vivo. *MBio*, 1(4):e00199–10, 2010. (Cited on page 2.)

[17] David E Geller, William H Pitlick, Pasqua A Nardella, William G Tracewell, and Bonnie W Ramsey. Pharmacokinetics and bioavailability of aerosolized tobramycin in cystic fibrosis. *CHEST Journal*, 122(1):219–226, 2002. (Cited on page 2.)

[18] Luis Gonzalez 3rd and Jeanne P Spencer. Aminoglycosides: a practical review. *Am. Fam. Physician*, 58(8):1811–1820, 1998. (Cited on page 2.)

[19] Karishma S. Kaushik, Ashley Kessel, Nalin Ratnayeke, and Vernita D. Gordon. A low-cost, hands-on module to characterize antimicrobial compounds using an interdisciplinary, biophysical approach. *PLoS Biol*, 13(1):e1002044, 01 2015. (Cited on pages 2 and 24.)

[20] Alejandro A Pezzulo, Xiao Xiao Tang, Mark J Hoegger, Mahmoud H Abou Alaiwa, Shyam Ramachandran, Thomas O Moninger, Phillip H Karp, Christine L Wohlford-Lenane, Henk P Haagsman, Martin van Eijk, et al. Reduced airway surface ph impairs bacterial killing in the porcine

cystic fibrosis lung. *Nature*, 487(7405):109–113, 2012. (Cited on pages 3 and 53.)

[21] Gerald B Pier. The challenges and promises of new therapies for cystic fibrosis. *The Journal of experimental medicine*, 209(7):1235–1239, 2012. (Cited on pages 3 and 53.)

[22] Karishma S. Kaushik, Nalin Ratnayeke, Parag Katira, and Vernita D. Gordon. The spatial profiles and metabolic capabilities of microbial populations impact the growth of antibiotic-resistant mutants. *J. R. Soc. Interface*, page 20150018, 2015. (Cited on pages 9, 15, 16, 21, 23, 25, 26, 28, 30, 31, 32, 34, 35, 36, 39, 40, 41, 49, 50, and 59.)

[23] W. Kirby, G. Yoshihara, K. Sundsted, and J. Warren. Clinical usefulness of a single disc method for antibiotic sensitivity testing. *Antibiotics Annual*, pages 892–897, 1955. (Cited on page 14.)

[24] K. Cooper. Theory of antibiotic inhibition zones in agar media. *Nature*, 1955. (Cited on pages 15 and 16.)

[25] Frederick Kavanagh et al. *Analytical microbiology.* New York and London: Academic Press, 1963. (Cited on pages 16 and 17.)

[26] R. K. Finn. Theory of agar diffusion methods for bioassay. *Anal. Chem.*, 31(6):975–977, 1959. (Cited on page 16.)

[27] A. Linton. Influence of inoculum size on antibiotic assays by the agar diffusion technique with klebsiella pneumoniae and streptomycin. *J. Bacteriol.*, 76(1):94, 1958. (Cited on pages 16, 17, and 19.)

[28] Xingyan Wu, Yue Guan, Gan Wei, and Henry Y Wang. Theoretical equations for agar-diffusion bioassay. *Industrial & engineering chemistry research*, 29(8):1731–1734, 1990. (Cited on page 17.)

[29] Christopher S Hayes, Stephanie K Aoki, and David A Low. Bacterial contact-dependent delivery systems. *Annual review of genetics*, 44:71–90, 2010. (Cited on page 25.)

[30] Ashish A Sawant, N Carol Casavant, Douglas R Call, and Thomas E Besser. Proximity-dependent inhibition in escherichia coli isolates from cattle. *Applied and environmental microbiology*, 77(7):2345–2351, 2011. (Cited on page 25.)

[31] Douglas A Treco and Fred Winston. Growth and manipulation of yeast. *Current Protocols in Molecular Biology*, pages 13–2, 2001. (Cited on page 33.)

[32] Jack T Pronk, H Yde Steensma, and JOHANNES P Van Dijken. Pyruvate metabolism in saccharomyces cerevisiae. *Yeast*, 12(16):1607–1633, 1996. (Cited on pages 38 and 52.)

[33] Fintan Moriarty, Joseph Elborn, and Michael Tunney. Effect of ph on the antimicrobial susceptibility of planktonic and biofilm-grown clinical pseudomonas aeruginosa isolates. *Br. J. Biomed. Sci.*, 64(3):101–104, 2006. (Cited on page 38.)

[34] David Lebeaux, Ashwini Chauhan, Sylvie Létoffé, Frédéric Fischer, Hilde de Reuse, Christophe Beloin, and Jean-Marc Ghigo. ph-mediated potentiation of aminoglycosides kills bacterial persisters and eradicates in vivo biofilms. *J. Infect. Dis.*, page jiu286, 2014.

[35] Harry W Taber, John Mueller, Paul Miller, and Amy Arrow. Bacterial uptake of aminoglycoside antibiotics. *Microbiol. Rev.*, 51(4):439, 1987. (Cited on page 38.)

[36] Steve P Bernier, Sylvie Létoffé, Muriel Delepierre, and Jean-Marc Ghigo. Biogenic ammonia modifies antibiotic resistance at a distance in physically separated bacteria. *Mol. Microbiol.*, 81(3):705–716, 2011. (Cited on page 38.)

[37] Dianne Damper and Wolfgang Epstein. Role of the membrane potential in bacterial resistance to aminoglycoside antibiotics. *Antimicrob. Agents Chemother.*, 20(6):803–808, 1981. (Cited on pages 43 and 46.)

[38] Robert A Quinn, Yan Wei Lim, Heather Maughan, Douglas Conrad, Forest Rohwer, and Katrine L Whiteson. Biogeochemical forces shape the composition and physiology of polymicrobial communities in the cystic fibrosis lung. *mBio*, 5(2):e00956–13, 2014. (Cited on page 52.)

[39] Kelli L Palmer, Lindsay M Aye, and Marvin Whiteley. Nutritional cues control pseudomonas aeruginosa multicellular behavior in cystic fibrosis sputum. *J. Bacteriol.*, 189(22):8079–8087, 2007. (Cited on page 52.)

[40] Stephen R Thomas, Anjana Ray, Margaret E Hodson, and Tyrone L Pitt. Increased sputum amino acid concentrations and auxotrophy of-pseudomonas aeruginosa in severe cystic fibrosis lung disease. *Thorax*, 55(9):795–797, 2000. (Cited on page 52.)

Part IV

APPENDICES

A

MATERIALS AND METHODS

The following are the complete materials and methods for this work. These descriptions are adapted from the Materials and Methods section of Kaushik et al. [22]

A.1 BACTERIAL STRAINS

P. aeruginosa PA14 was used as the wild-type (WT) strain (gift from the lab of Marvin Whiteley, UT Austin). To generate spontaneous antibiotic-resistant mutants, WT PA14 cells were grown overnight in antibiotic-free media and aliquots of overnight cultures were plated on agar containing 8 μg/mL tobramycin. Resistant mutant colonies (at most $1-2$ per plate) that grew were picked and re-grown for archiving and subsequent experiments. Strains were archived by mixing 0.25 mL of glycerol (100% v/v) with 0.75 mL of the overnight culture (20-30% final glycerol concentration) and stored at −80°C. Upon subsequent plating, strains that showed evidence of mixed colony types were isolated again by overnight cultures and freezing.

To generate antibiotic-resistant mutants in the presence of antibiotic, WT PA14 cells were passaged in increasing tobramycin concentrations (0.3, 0.6, 1.2, 1.8, 2.4, 3.0, 3.6, 4.2 μg/mL) for eight successive days. Each day, culture aliquots were frozen as described previously.

Transposon-insertion loss-of-function mutants were obtained from the PA14 non redundant transposon library for use in knockout experiments. *P. aeruginosa* strain PAO1, seventeen clinical *Pseudomonas* isolates, *Pseudomonas* sandgrass isolate, *P. fluorescens*, Methicillin-resistant *S. aureus* Mu50, *E. coli* DH5α, *Burkholderia cepacia* and Δ*phz1/2* mutant (gifts from the Whiteley lab, UT Austin), *Serratia marcescens* (gift from the lab of Rasika Harshey, UT Austin) and the yeast strain *Saccharomyces cerevisiae* S288C (gift from the lab of Edward Marcotte, UT Austin)

A.1.1 *Culture conditions*

All bacterial strains were grown in Luria-Bertani (LB) broth or on LB agar except where otherwise indicated. For LB broth and agar, we used Miller's formulation containing 0.5% yeast extract, 1% tryptone, and 1% sodium chloride for broth, with 1.2% agar for plates. All liquid cultures were grown at 37°C, except for *P. fluorescens* and *Burkholderia cepacia* which were grown at 30ºC (their

optimum temperature for growth). *Saccharomyces cerevisiae* was grown in Yeast-Peptone-Dextrose (YPD) broth or agar except where otherwise indicated. YPD consists of 1% yeast extract, 2% tryptone, and 2% dextrose for broth, with 1.2% agar for plates. *S. cerevisiae* liquid cultures were grown at 30°C. Overnight liquid cultures were incubated under shaking conditions (180 rpm) for $16-18$ hours. When indicated, LB or YPD agar was incorporated with the antibiotics tobramycin (Indofine Chemical Company, NJ) or gentamicin (Fisher Scientific, NJ). Except when indicated otherwise, the tobramycin and gentamicin concentrations used whereas 8 μg/mL.

A.1.2 *Stability of antibiotic-resistant mutants*

To test the stability of the antibiotic-resistant mutants that we generated, we passaged strains for three successive days in antibiotic-free LB broth, following which aliquots of cultures were plated on antibiotic-containing LB agar (LB-tobramycin or gentamicin 8 μg/mL). Confluent lawns of bacteria grew on the antibiotic agar, which indicated that antibiotic-resistant mutants had retained their resistance even in the absence of selection.

A.1.3 *Minimum inhibitory concentration (MIC) measurements*

MIC for antibiotics was measured (in triplicate) in LB broth for the different bacterial strains and in YPD broth for the yeast strain using the broth microdilution method based on CLSI guidelines.

A.2 EXPERIMENTS IN SPATIALLY-MIXED SYSTEMS

WT PA14 cells of varying numbers ($\sim 10^6 - 10^{11}$ cells) were mixed in 3 mL of 0.6% LB agar and overlaid on antibiotic-containing agar (LB-tobramycin 4 μg/mL). Number of cells was calculated by measuring optical density (OD600) of the overnight cultures (Nanodrop 2000c spectrophotometer, Thermo Scientific) followed by conversion using the conversion factor OD 1 corresponds to 0.8×10^9 cells/mL. Plates were incubated at 37°C for 48 hours following which numbers of antibiotic-resistant colonies were counted using ImageJ v.1.47.

A.3 DISC-DIFFUSION ASSAY FOR SPATIALLY-STRUCTURED SYSTEMS

To perform the disc diffusion assay, we required uniform lawns of antibiotic-resistant mutants on the surface of the agar. When antibiotic-resistant cells were spread directly on the antibiotic-containing agar (LB-tobramycin 8 μg/mL agar) surface, we observed a marked reduction in the numbers of mutant colonies that survived and grew, resulting in a non-uniform lawn. To overcome

this, we used an "overlay agar technique" to lay down the antibiotic-resistant mutant lawn. Antibiotic-resistant mutants from overnight cultures ($\sim 10^8$ cells, unless otherwise stated) were added to 3 mL of 0.6% (soft) LB agar and overlaid on antibiotic-containing LB agar (tobramycin or gentamicin at 8 μg/mL).

For deposition on the filter discs, overnight, stationary-phase cultures (32 mL) were centrifuged to form a pellet (4000 rpm, 20 min) and washed by removing supernatant and adding sterile media. This was done three times before resuspension in 100 μl of fresh, sterile LB broth. From this, 10 μl ($\sim 10^9 - 10^{10}$ cells for bacterial cultures, $\sim 10^{11} - 10^{12}$ cells for yeast cultures, unless otherwise stated) was deposited on sterile 7-mm diameter filter discs (Whatman) placed on the agar surface. The number of cells was calculated by measuring optical density of the overnight culture (OD600) (Nanodrop 2000c spectrophotometer, Thermo Scientific) followed by conversion using the conversion factor OD 1 corresponds to 0.8×10^9 cells/mL for bacterial strains and 3×10^7 cells/mL for the yeast strain S. cerevisiae. Plates were incubated at 37°C for $24 - 48$ hours, after which the width of inhibition (X) was measured from the edge of the filter disc to the edge of the inhibition zone.

A.4 MODIFICATIONS OF THE DISC-DIFFUSION ASSAY

A.4.1 *Using antibiotic-free agar*

On antibiotic-free agar, the assay was modified such that serial ten-fold dilutions of antibiotic-resistant mutant lawns ($10^7 - 10^4$ cells) were overlaid on antibiotic-free LB agar, following which WT PA14 cells were deposited on the filter discs.

A.4.2 *Effect of antibiotic-resistant mutant lawn density*

Increasing densities of antibiotic-resistant mutants (1×10^2, 2×10^2, 4×10^2, 8×10^2 and 1.6×10^3 cells/nL) were overlaid on LB-tobramycin agar and increasing numbers of WT PA14 (1.4×10^8, 2.8×10^8, 5.6×10^8 and 1.2×10^9 cells) were deposited on filter discs. Plates were incubated at 37°C for $24 - 48$ hours and width of inhibition (X) were measured.

A.4.3 *Determining the role of antibiotic in inhibition*

We used a set of complementary experiments, the "antibiotic-free core" and "antibiotic-containing core" experiments, to determine the role of antibiotic in production and activity of the IF.

In the antibiotic-free core experiment, antibiotic-resistant mutants were overlaid on LB-tobramycin agar and cores of different diameters (7, 10 and 15-

mm) were created with a sterile metal punch. Wells were filled with antibiotic-free LB agar (1.2%) and allowed to set. As soon as the cores set (within 10 min), filter discs were placed on the antibiotic-free (LB) core and WT PA14 cells were deposited. As a control, WT cells were also deposited directly on a filter disc on the antibiotic-resistant mutant lawn (no core).

In the antibiotic-containing core experiment, decreasing ten-fold serial dilutions (10^7–10^4 cells) of antibiotic-resistant mutants was overlaid on antibiotic-free LB agar. Cores (7-mm diameter) were created in the agar, filled with LB-tobramycin agar (1.2%) and allowed to set. As soon as the cores set (within 10 min), filter-discs were placed on the LB-tobramycin core and WT PA14 cells were deposited.

A.4.4 *Test the role of nutrient depletion*

Antibiotic-resistant mutants were overlaid on LB-tobramycin agar and cores of LB-tobramycin agar (1.2%) containing single (normal) strength nutrients (0.5% yeast extract, 1% tryptone), double-strength nutrients (1% yeast extract, 2% tryptone), and ten-times nutrient strength (5% yeast extract, 10% tryptone). Filter discs were placed on the cores and WT PA14 cells were deposited. In addition, a core completely lacking nutrients (only 1.2% agar with tobramycin 8 μg/mL, no WT cells were deposited) was created, to simulate a nutrient sink.

A.4.5 *Using media devoid of nutrients*

Antibiotic-resistant mutants were overlaid on LB-tobramycin agar and cores of different diameters (7 and 10-mm) containing nutrient-free tobramycin agar (1.2%) were created. Filter discs were placed on the cores and WT PA14 cells were deposited. As controls, WT PA14 cells were also deposited on filter discs placed on cores of nutrient-containing LB-tobramycin agar and directly on the antibiotic-resistant lawn (no core).

A.4.6 *Using pH change to probe the nature of the released inhibitory factor*

Bromthymol blue (BTB) solution (stock solution 1 mg/mL) was added to nutrient-free tobramycin agar or LB-tobramycin agar at a final concentration of 0.002%. 32 mL of overnight cultures of different microbial strains were centrifuged (4000 rpm, 20 min) to form a pellet, washed (thrice) and resuspended in fresh, sterile LB broth (100 μL). 10 μL (~ 10^9–10^{10} cells) of this suspension were deposited on filter discs with and without antibiotic-resistant lawns in the overlay agar. The overlay agar had the same nutrient composition as the bulk agar below. Plates were incubated at 37 °C and observed every hour for an alkaline or acidic change around the filter discs. Images were taken immediately

after deposition (for nutrient-free BTB agar) or 2 hours after deposition (for LB-tobramycin BTB agar) or after overnight incubation (for antibiotic-resistant mutant lawns). Intensity profiles and width of alkaline change (X_c) were quantified using ImageJ v.1.47.

A.4.7 *Testing the effect of different nutrient conditions of overnight growth media on inhibition*

P. aeruginosa WT PA14, *S. aureus*, *E. coli* and the yeast strain *S. cerevisiae* were grown overnight under shaking conditions in LB broth and in YPD broth. All cultures were incubated at 37°C except for the yeast strain *S. cerevisiae* that was grown at 30°C. After $16-18$ hours of overnight growth, optical densities (OD600) of the overnight cultures were measured. In LB and YPD medium, WT PA14, *S. aureus* and *E. coli* grew to a density of ~10^9 cells / mL. In YPD medium, *S. cerevisiae* grew to a density of ~10^8 cells / mL. As expected, *S. cerevisiae* grew poorly in LB medium (as compared to YPD) with a density of ~10^7 cells / mL. The pH of the cell cultures and of filter-sterilized supernatant from these cultures was measured using pH indicator strips (Cardinal Health, IL). Cells were filtered out of the supernatant using a 0.2 μm syringe filter.

Overnight cultures were centrifuged (4000 rpm, 20 min), washed (thrice) and resuspended in fresh, sterile LB or YPD broth (100 μL). Of this resuspended culture, ~10^9 cells were deposited on filter discs on nutrient-free tobramycin BTB agar, nutrient-containing LB tobramycin BTB agar, and LB-tobramycin agar overlaid with antibiotic-resistant mutants (~10^8 cells were spread to initiate the lawn). In addition, filter-sterilized supernatant from each culture condition and sterile, fresh LB and YPD broth were also deposited onto filter discs. Plates were incubated at 37°C and observed every hour for an alkaline or acidic change around the filter discs. Images were taken immediately after deposition (for nutrient-free BTB agar), 2 hours after deposition (for LB-tobramycin BTB agar) or after overnight incubation (for LB-tobramycin agar with antibiotic-resistant mutant lawns). Intensity profiles were quantified using ImageJ v.1.47.

A.4.8 *Deposition of exogenous alkali compounds*

10 μL of ammonium hydroxide (NH_4OH) (14.8M, 7.4M, 4.9M, 3.7M, 2.9M, 2.4M), sodium hydroxide (NaOH) (1M, 0.5M, 0.33M, 0.25M, 0.2M), sodium bicarbonate ($NaHCO_3$) (1M, 0.5M, 0.33M, 0.25M, 0.2M) and 1M ammonium chloride (NH_4Cl) were deposited on antibiotic-resistant mutant lawns overlaid on LB-tobramycin 8 μg/mL agar with and without BTB. Plates were incubated at 37°C. LB-tobramycin BTB agar was observed hourly for alkaline or acidic change. LB-tobramycin agar overlaid with antibiotic-resistant mutants

was incubated for $24-48$ hours, following which widths of inhibition (X) were measured. Images were taken 2 hours after deposition (for BTB agar) or after overnight incubation (for LB-tobramycin agar with antibiotic-resistant mutant lawns). Intensity profiles and width of alkaline change (X_c) were quantified using ImageJ v.1.47. 10 µL of exogenous alkali compounds (2.1M NH_4OH, 0.5M NaOH and 0.5M $NaHCO_3$) were also deposited on decreasing dilutions ($10^8 - 10^5$ cells) antibiotic-resistant mutant lawns overlaid on antibiotic-free LB agar.

A.4.9 *Supernatant assays*

Filter-sterilized supernatant (10 µL, sterilized using a 0.2 µm syringe filter) from overnight, stationary-phase cultures of WT PA14 cells was deposited on filter discs on nutrient-free tobramycin BTB agar and LB-tobramycin BTB agar. Supernatant (10 µL) was also deposited on antibiotic-resistant mutant lawns on LB-tobramycin agar. BTB plates were observed hourly for an alkaline change. Plates overlaid with antibiotic-resistant lawns were incubated at 37°C for $24-48$ hours, following which widths of inhibition (X) were measured. Images were taken 2 hours after deposition (for LB-tobramycin BTB agar) or after overnight incubation (for LB-tobramycin agar with antibiotic-resistant mutant lawns). Intensity profiles and widths of alkaline change (X_c) were quantified using ImageJ v.1.47.

A.5 DETECTION OF AMMONIA AND/OR AMINE EMISSION

An ion-selective electrode (Orion 920A, Thermo Scientific) was used to detect ammonia or amine emission. LB-tobramycin agar was poured into 20 mL sterile, narrow-necked glass vials such that the vials were almost filled to capacity. This reduced the headspace available between the upper meniscus of the agar and cap of the vial, preventing the dilution of released products. Cells were deposited on the filter discs placed on the upper surface of the agar and the vials were immediately capped. The electrode was calibrated using 0.1, 0.5, 1, 2.5 and 5 mg/L concentrations of ammonium sulfate (stock solution 500 mg/L) added to distilled water. While measuring ammonia levels for calibration and in the experiment vials, the electrode was held at a distance of 1 cm. above the upper surface of the media (gaseous phase). All measurements were conducted with the samples placed on a hot plate set at 37°C. Using standard calibration curves, ammonia emission levels were determined.

A.6 STATISTICAL METHODS

All statistical tests were either performed using R v2.15.2, or Microsoft Excel. Linear regressions performed for modeling of the disc-diffusion assay, and nonlinear regressions for modeling of inhibition in mixed systems were performed using least squares algorithms. All stated error bounds in values and on graphs are one standard error unless otherwise stated, and were propagated using standard statistical methods. Correlation statistics and Student t tests were done in Microsoft Excel.